AEM
Journals.ASM.org

Steroid Hydroxylation by Basidiomycete Peroxygenases: a Combined Experimental and Computational Study

Esteban D. Babot,[a] José C. del Río,[a] Marina Cañellas,[b,c] Ferran Sancho,[b,c] Fátima Lucas,[b] Víctor Guallar,[b,d] Lisbeth Kalum,[e] Henrik Lund,[e] Glenn Gröbe,[f] Katrin Scheibner,[f] René Ullrich,[g] Martin Hofrichter,[g] Angel T. Martínez,[h] Ana Gutiérrez[a]

Instituto de Recursos Naturales y Agrobiología de Sevilla, CSIC, Seville, Spain[a]; Joint BSC-CRG-IRB Research Program in Computational Biology, Barcelona Supercomputing Center, Barcelona, Spain[b]; Anaxomics Biotech, Barcelona, Spain[c]; ICREA, Barcelona, Spain[d]; Novozymes A/S, Bagsvaerd, Denmark[e]; JenaBios GmbH, Jena, Germany[f]; TU Dresden, Department of Bio- and Environmental Sciences, Zittau, Germany[g]; Centro de Investigaciones Biológicas, CSIC, Madrid, Spain[h]

The goal of this study is the selective oxyfunctionalization of steroids under mild and environmentally friendly conditions using fungal enzymes. With this purpose, peroxygenases from three basidiomycete species were tested for the hydroxylation of a variety of steroidal compounds, using H_2O_2 as the only cosubstrate. Two of them are wild-type enzymes from *Agrocybe aegerita* and *Marasmius rotula*, and the third one is a recombinant enzyme from *Coprinopsis cinerea*. The enzymatic reactions on free and esterified sterols, steroid hydrocarbons, and ketones were monitored by gas chromatography, and the products were identified by mass spectrometry. Hydroxylation at the side chain over the steroidal rings was preferred, with the 25-hydroxyderivatives predominating. Interestingly, antiviral and other biological activities of 25-hydroxycholesterol have been reported recently (M. Blanc et al., Immunity 38:106–118, 2013, http://dx.doi.org/10.1016/j.immuni.2012.11.004). However, hydroxylation in the ring moiety and terminal hydroxylation at the side chain also was observed in some steroids, the former favored by the absence of oxygenated groups at C-3 and by the presence of conjugated double bonds in the rings. To understand the yield and selectivity differences between the different steroids, a computational study was performed using Protein Energy Landscape Exploration (PELE) software for dynamic ligand diffusion. These simulations showed that the active-site geometry and hydrophobicity favors the entrance of the steroid side chain, while the entrance of the ring is energetically penalized. Also, a direct correlation between the conversion rate and the side chain entrance ratio could be established that explains the various reaction yields observed.

Steroids represent an important class of natural compounds that are widespread in nature and have a multitude of pharmacological properties. Indeed, steroids are ranked among the most marketed medical products and represent the second largest category next to antibiotics. The physiological activity of steroids depends on their structures, including the oxidation state of the rings, and the type, number, and regio- and stereoposition of the functional groups attached (1). It is known that even minor changes in the structure of steroids can highly affect their biological activity, which has promoted countless studies on the modification of naturally occurring steroids in search of new and more active compounds (2). Among these modifications, hydroxylation is one of the most important reactions in steroid oxyfunctionalization.

Hydroxylation serves to increase the polarity of the rather hydrophobic steroids, and hydroxylated steroids often express a higher level of biological activity than their less polar nonhydroxylated analogs. Moreover, hydroxylation can be used to develop intermediates for further synthesis by offering access to otherwise inaccessible sites of the steroid molecule. These modifications have been obtained mostly by applying microorganisms (1), with only a few examples where isolated enzymes were used. Members of the cytochrome P450 monooxygenase (P450) superfamily are notable examples of such enzymatic catalysts, since, because of their catalytic versatility, they would perfectly meet the requirements of chemical synthesis (3, 4). However, large-scale applications are not yet feasible due to the intrinsic properties of these oxygenases (5), whose activation requires NAD(P)H as an electron donor and auxiliary flavin-reductases (or a second flavin domain) for electron transfer to O_2 (6).

A few years ago, a new peroxidase type was discovered in the wood-dwelling basidiomycete *Agrocybe aegerita* (7), which turned out to be a true peroxygenase efficiently transferring oxygen from peroxide to various organic substrates (8). This peroxygenase is able to catalyze reactions formerly assigned only to P450s (9). However, unlike P450s, which are intracellular enzymes whose activation often requires an auxiliary enzyme and a source of reducing power, the *A. aegerita* enzyme is a secreted protein; therefore, it is far more stable and requires only H_2O_2 for activation (8). The *A. aegerita* peroxygenase has been shown to catalyze numerous interesting oxygenation reactions on aromatic compounds (10), and recently, the action of this enzyme on aliphatic compounds was demonstrated, expanding its biotechnological interest (11, 12). The enzyme, first described as a haloperoxidase and

Received 27 February 2015 **Accepted** 3 April 2015
Accepted manuscript posted online 10 April 2015
Citation Babot ED, del Río JC, Cañellas M, Sancho F, Lucas F, Guallar V, Kalum L, Lund H, Gröbe G, Scheibner K, Ullrich R, Hofrichter M, Martínez AT, Gutiérrez A. 2015. Steroid hydroxylation by basidiomycete peroxygenases: a combined experimental and computational study. Appl Environ Microbiol 81:4130–4142. doi:10.1128/AEM.00660-15.
Editor: J. L. Schottel
Address correspondence to Ana Gutiérrez, anagu@irnase.csic.es.
Supplemental material for this article may be found at http://dx.doi.org/10.1128/AEM.00660-15.

doi:10.1128/AEM.00660-15

later mostly referred to as aromatic peroxygenase (APO), now is named "unspecific peroxygenase" (UPO; EC 1.11.2.1).

After the first peroxygenase of *A. aegerita* (7), similar enzymes also have been found in other basidiomycetes, such as *Coprinellus radians* (13) and *Marasmius rotula* (14), and there are indications for their widespread occurrence in the fungal kingdom (15). Recently, over 100 peroxygenase-type genes (encoding enzymes of the heme-thiolate peroxidase superfamily) have been identified during the analysis of 24 basidiomycete genomes (16), including *Coprinopsis cinerea* (17). The wild-type *C. cinerea* peroxygenase has not been isolated to date from this fungus, but one of the peroxygenase genes from its genome (protein model 7249, available from the Joint Genome Institute [JGI; http://genome.jgi.doe.gov/Copci1]) was heterologously expressed by Novozymes A/S (Bagsvaerd, Denmark). This first recombinant peroxygenase can be a powerful biocatalyst for synthetic applications because of the potentially high expression yield and the possibility of tuning its catalytic and operational properties using protein engineering tools. Recently, the ability of this recombinant peroxygenase in the oxyfunctionalization of several aliphatic compounds was demonstrated (18).

Here, the efficiency of three different peroxygenases, namely, the wild enzymes from *A. aegerita* (*Aae*UPO) and *M. rotula* (*Mro*UPO) and the recombinant enzyme from *C. cinerea* (r*Cci*UPO), in oxyfunctionalization of a variety of steroidal compounds (including free and esterified sterols, steroid hydrocarbons, and ketones) is evaluated for the first time. All three fungi are agaric basidiomycetes, but they belong to different families of the order *Agaricales*, and they also differ to some extent from an ecophysiological point of view. *M. rotula* (family *Marasmiaceae*) is a fungus that stands between white rotters and litter decomposers, because it preferably colonizes small twigs of broad-leaved trees (*Fagus*, *Quercus*, and *Acer*). *C. cinerea* (family *Psathyrellaceae*) naturally dwells on older dung and in soils rich in organic nitrogen (i.e., it is a specialized litter decomposer). *A. aegerita* (family *Bolbitaceae*) is a wood-dwelling fungus that causes an unspecific white rot on trunks and stumps of broad-leaved trees (e.g., *Populus* and *Acer* species). However, it would be daring to conclude from these evolutionary and ecological differences that the UPOs of these fungi must be different.

In addition to the experimental assays, where the products from the reaction of a variety of steroids with the three above-mentioned peroxygenases were analyzed by gas chromatography-mass spectrometry (GC-MS), a set of representative molecules was selected for computational simulations with *Aae*UPO (for which a crystal structure is available) to get further insights into the molecular determinants that affect the reactivity of the different steroid types. All simulations followed an identical protocol where, after appropriate preparation of the protein with heme as compound I [the two-electron oxidized cofactor containing an Fe(IV)=O porphyrin cation radical complex], each substrate was placed at the entrance of the heme access channel, still in the solvent. From there the substrate explored both the entrance pathway and the active site using Protein Energy Landscape Exploration (PELE) software (19, 20). From the information provided by the energy profiles and trajectories, analyses of the effect of the structural differences between the substrates and their peroxygenase reactivity could be rationalized.

MATERIALS AND METHODS

Enzymes. r*Cci*UPO was provided by Novozymes A/S (Bagsvaerd, Denmark). This recombinant enzyme corresponds to the protein model 7249 from the sequenced *C. cinerea* genome, available at the JGI (http://genome.jgi.doe.gov/Copci1), expressed in *Aspergillus oryzae* (40). The protein was purified using a combination of S-sepharose and SP-sepharose ion-exchange chromatography. The recombinant peroxygenase preparation is an electrophoretically homogeneous glycoprotein with a molecular mass of around 44 kDa (a nonuniform glycosylation pattern was observed), a typical UV-visible (UV-Vis) spectrum with a Soret band at 418 nm, and the ability to oxygenate different aromatic compounds with a specific activity of approximately 100 U · mg^{-1} (measured as described below).

The *Aae*UPO and *Mro*UPO enzymes are two wild-type peroxygenases isolated from cultures of *A. aegerita* DSM 22459 and *M. rotula* DSM 25031, deposited at the German Collection of Microorganisms and Cell Cultures (Braunschweig, Germany). *Aae*UPO was produced in suspensions of soybean meal and purified by several steps of fast protein liquid chromatography (FPLC) using different ion exchangers (SP-sepharose, MonoQ, and MonoS) with size exclusion chromatography (Superdex 75) as the final isolation step. The final protein fraction had a molecular mass of 46 kDa with one enriched isoform (*Aae*UPO II). This isoform was used in the present study (7, 21). *Mro*UPO was purified by FPLC to apparent homogeneity, confirmed by sodium dodecyl sulfate-polyacrylamide gel electrophoresis (SDS-PAGE) under denaturing conditions, and showed a molecular mass of 32 kDa and an isoelectric point of pH 5.0 to 5.3. The UV-visible spectra of the enzymes showed a characteristic maximum around 420 nm (Soret band of heme-thiolate proteins) (14).

All media and columns used for enzyme isolation were purchased from GE Healthcare Life Sciences. One UPO activity unit is defined as the amount of enzyme oxidizing 1 μmol of veratryl alcohol to veratraldehyde (ε_{310}, 9,300 $M^{-1} \cdot cm^{-1}$) in 1 min at 24°C, pH 7 (the optimum for peroxygenase activity), after addition of H_2O_2 (0.5 mM H_2O_2 in r*Cci*UPO reaction mixtures and 2.5 mM H_2O_2 in *Aae*UPO and *Mro*UPO reaction mixtures).

Steroids. The model steroid compounds (from Sigma-Aldrich) used in the enzymatic reactions include (i) free sterols, such as cholesterol, campesterol, ergosterol, sitosterol, and stigmasterol; (ii) steroid ketones, such as cholestan-3-one, 4-cholesten-3-one, cholesta-3,5-dien-7-one, and testosterone; (iii) steroid hydrocarbons, such as cholestane, cholesta-3,5-diene, and pregnane; and (iv) sterol esters, such as cholesteryl acetate, cholesteryl butyrate, and cholesteryl caprylate (see Fig. 1).

Enzymatic reactions. Reactions of the model steroids (0.05 mM concentration) with the three peroxygenases (1 U) were performed in 5-ml vials containing 50 mM sodium phosphate (pH 7 in *Aae*UPO and r*Cci*UPO reactions and pH 5.5 in *Mro*UPO reactions) at 40°C and a 60-min reaction time in the presence of H_2O_2 (0.5 mM in r*Cci*UPO reactions and 2.5 mM in *Aae*UPO and *Mro*UPO reactions). Prior to use, the substrates were dissolved in acetone and added to the buffer to give a final acetone concentration of 40% (vol/vol) in most cases. In control experiments, substrates were treated under the same conditions (including 0.5 mM and 2.5 mM H_2O_2) but without enzyme. Products were recovered by liquid-liquid extraction with methyl *tert*-butyl ether and dried under N_2. *N*,*O*-Bis(trimethylsilyl)trifluoroacetamide (Supelco) was used to prepare trimethylsilyl (TMS) derivatives that were analyzed by GC-MS.

GC-MS analyses. The GC-MS analyses were performed with a Varian 3800 chromatograph coupled to an ion-trap detector (Varian 4000) using a medium-length fused-silica DB-5HT capillary column (12 m by 0.25 mm internal diameter, 0.1 μm film thickness) from J&W Scientific (22). The oven was heated from 120°C (1 min) to 300°C (15 min) at 10°C · min^{-1}. The injector was programmed from 60°C (0.1 min) to 300°C (28 min) at 200°C · min^{-1}. The transfer line was kept at 300°C, and helium was used as the carrier gas (2 ml · min^{-1}). For some analyses, a Shimadzu GC-MS QP2010 Ultra with a fused-silica DB-5HT capillary column (30 m

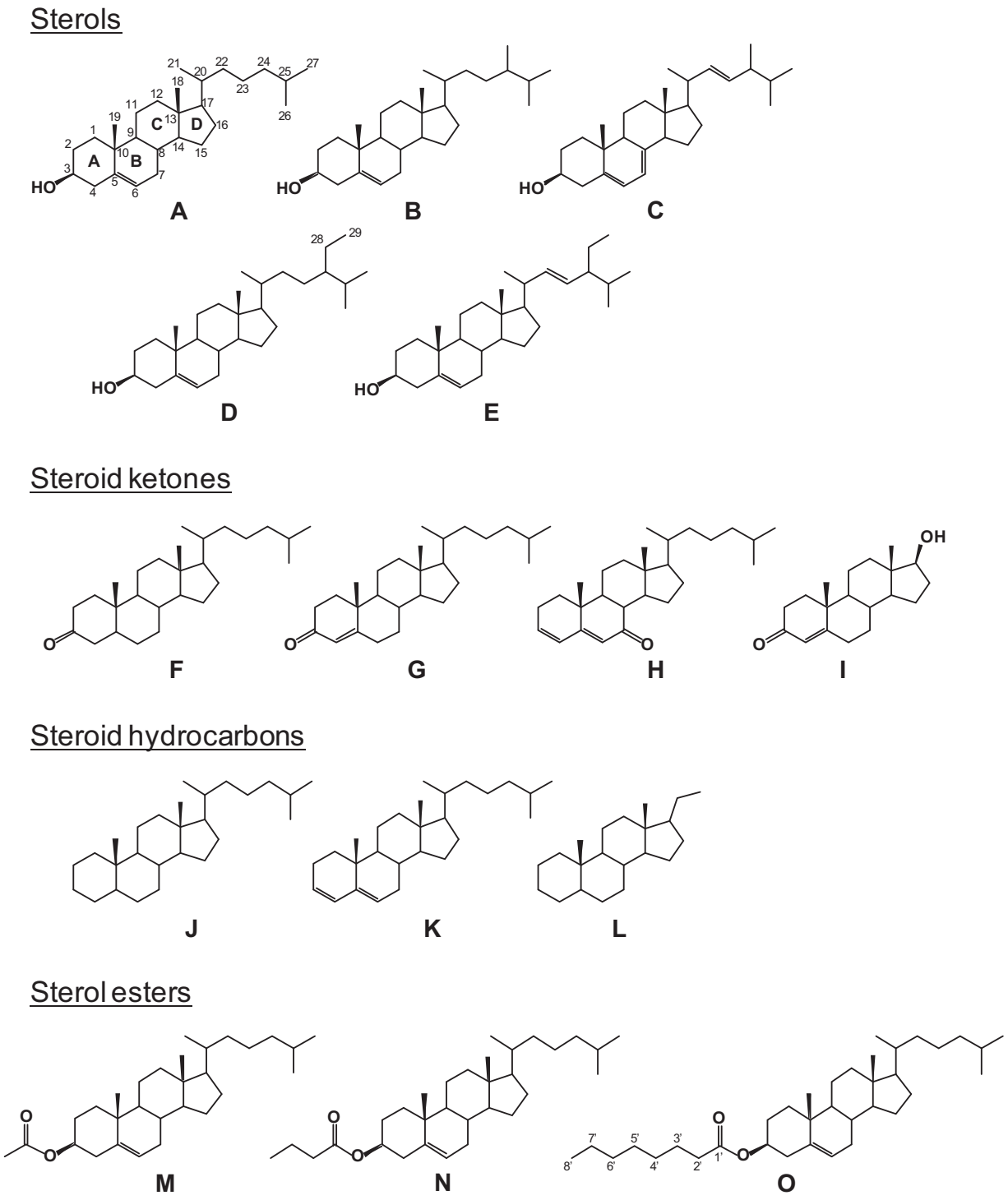

FIG 1 Chemical structures of the different steroid compounds tested as substrates of the peroxygenases, including (i) free sterols, such as cholesterol (A), campesterol (B), ergosterol (C), sitosterol (D), and stigmasterol (E); (ii) steroid ketones, such as cholestan-3-one (F), 4-cholesten-3-one (G), cholesta-3,5-dien-7-one (H), and testosterone (I); (iii) steroid hydrocarbons, such as cholestane (J), cholesta-3,5-diene (K), and pregnane (L); and (iv) sterol esters, such as cholesteryl acetate (M), cholesteryl butyrate (N), and cholesteryl caprylate (O).

by 0.25 mm internal diameter, 0.1 μm film thickness) also was used. The oven was heated from 120°C (1 min) to 300°C (15 min) at 5°C · min^{-1}. The injection was performed at 300°C, and the transfer line was kept at 300°C. Compounds were identified by mass fragmentography and comparing their mass spectra with those of the Wiley and NIST libraries and standards. Quantification was obtained from total-ion peak area, using response factors of the same or similar compounds. Data from replicates were averaged, and in all cases (substrate conversion and relative abun-

dance of reaction products) the standard deviations were below 3.5% of the mean values.

PELE computational analyses. For the computational study, eight representative compounds (cholesterol, sitosterol, cholestan-3-one, cholesta-3,5-dien-7-one, cholestane, cholesta-3,5-diene, cholesteryl acetate, and cholesteryl caprylate) were prepared and PELE simulations performed.

The starting structure for all PELE simulations was the *Aae*UPO 2.19-Å-resolution crystal (PDB entry 2YOR) (23). As the optimum pH for peroxygenase activity is 7, the structure was prepared accordingly using Schrodinger's Protein Preparation Wizard (24) and H++ web server (25). Histidines were δ-protonated, with the exception of His-82 (ε-protonated) and His-118 and His-251 (double protonated). All acidic residues were deprotonated, except Asp-85, which was kept in its protonated state. The eight ligands studied in this section were optimized with Jaguar 7.8 (Schrödinger, LLC, New York, NY) at the DFT/M06 level with the 6-31G** basis and a PBF implicit solvent in order to obtain their electrostatic potential atomic charges. Finally, the heme site was modeled as compound I after being fully optimized in the protein environment with quantum mechanics/molecular mechanics (QM/MM) using QSite 5.7 (Schrödinger).

Once the initial protein structure was prepared, the optimized ligands were placed manually in identical positions at the entrance of the protein's binding pocket and PELE (20) simulations were performed. PELE is a Monte Carlo-based algorithm that produces new configurations through a sequential ligand and protein perturbation, side-chain prediction, and minimization steps. New configurations then are filtered with a Metropolis acceptance test, where the energy is described with an all-atom OPLS force field (26) and a surface-generalized Born solvent (27). In this way it is possible to locate and characterize local and global minima structures for the most favorable protein-ligand interactions. PELE has been used successfully in a number of ligand migration studies with both small and large substrates (28–30). In this work, PELE was set up first to drive the ligands inside the protein until the center of mass was less than 10 Å from the compound I oxygen. After that, simulation proceeded by allowing a free exploration of the enzyme active site by the ligand. The results presented are based on ~350 48-h trajectories for each ligand.

RESULTS

The efficiency of three peroxygenases (*Aae*UPO, *Mro*UPO, and r*Cci*UPO) hydroxylating 15 steroidal compounds (including free and esterified sterols, steroid hydrocarbons, and ketones) was experimentally evaluated, and the reaction products were analyzed by GC-MS. To rationalize the results obtained with the different steroid types, substrate diffusion simulations were performed with PELE (20), providing energy profiles and ligand trajectories, as described in the final section.

Free sterol reactions. Free C_{27} (cholesterol), C_{28} (campesterol and ergosterol), and C_{29} (sitosterol and stigmasterol) sterols (Fig. 1A to E, respectively) were tested as UPO substrates (Table 1). Cholesterol was converted to a larger extent than the other sterols, although the individual enzymes showed differences in their performance (after 60 min): r*Cci*UPO completely (100%) transformed the substrate, followed by *Aae*UPO (64%) and *Mro*UPO (23%). The reaction products of cholesterol were oxygenated derivatives at the C-24, C-25, and C-26/C-27 positions of the side chain (Fig. 1 depicts atom numbering), with the monohydroxylated C-25 derivative predominating (Table 2). Interestingly, a strict regioselectivity was observed in the reaction of cholesterol with r*Cci*UPO, yielding 25-hydroxycholesterol as the sole reaction product.

The position of the hydroxyl group was determined by the mass spectra of the TMS derivatives, as found for 25-hydroxycholesterol (see Fig. S1 in the supplemental material). The spectrum includes the molecular ion (*m/z* 546) and a characteristic ion at *m/z* 131, resulting from C-24–C-25 bond cleavage, together with additional fragments. Likewise, the spectra of monohydroxylated derivatives at C-24 and C-26 (not shown) showed, in addition to the molecular ion at *m/z* 546, the characteristic fragment at *m/z* 131, described above, and that at *m/z* 145 from the C-23–C-24 bond cleavage. In the *Aae*UPO and *Mro*UPO reactions, further oxidized compounds (carboxycholesterol) at C-26/C-27 were identified (with a molecular ion at *m/z* 560 and the above-described characteristic fragment at *m/z* 145), although they were in small amounts.

TABLE 1 Conversion of different types of steroid compounds by the r*Cci*UPO, *Aae*UPO, and *Mro*UPO peroxygenases within a 60-min reaction

Substrate	% substrate transformed by:		
	r*Cci*UPO	*Aae*UPO	*Mro*UPO
Free sterols			
Cholesterol	100	64	23
Campesterol	30	47	10
Ergosterol	6	10	7
Sitosterol	6	13	4
Stigmasterol	2	2	5
Steroid ketones			
Cholestan-3-one	54	42	12
4-Cholesten-3-one	100	67	14
Cholesta-3,5-dien-7-one	97	57	39
Testosterone	0	0	0
Steroid hydrocarbons			
Cholestane	14	3	1
Cholesta-3,5-diene	34	18	23
Pregnane	0	0	37
Sterol esters			
Cholesteryl acetate	34	16	5
Cholesteryl butyrate	7	1	1
Cholesteryl caprylate	0	0	0

The C_{28} sterols, especially ergosterol, were transformed to a lesser extent than cholesterol (Table 1). *Aae*UPO showed more reactivity toward campesterol and ergosterol than the other peroxygenases. The reaction of ergosterol was strictly regioselective, with 25-hydroxyergosterol being the only reaction product identified in all cases (Table 2). The reaction with campesterol also was highly regioselective, giving the 25-hydroxyderivative as the main product, although hydroxylation at C-26 also was observed (especially in the r*Cci*UPO reaction). Likewise, the three peroxygenases showed low reactivity with the C_{29} sterols, and only very low conversion rates (<13%) were attained (Table 1). In the reaction with stigmasterol, only the monohydroxylated derivative at C-25 was observed, whereas with sitosterol, nearly the same amount of 28-hydroxysitosterol was formed by r*Cci*UPO (and a small amount by *Aae*UPO) (Table 2).

Steroid ketone reactions. Cholestan-3-one, 4-cholesten-3-one, cholesta-3,5-dien-7-one, and testosterone (Fig. 1F to I, respectively) were tested as UPO substrates (Table 1). r*Cci*UPO was the most efficient enzyme in transforming steroid ketones except testosterone, which was not modified by any of the three peroxy-

genases, followed by *Aae*UPO and *Mro*UPO. The unsaturated 4-cholesten-3-one and cholesta-3,5-dien-7-one were completely transformed by r*Cci*UPO, and the saturated cholestan-3-one also was significantly transformed (54%).

The three ketones were predominantly monohydroxylated at C-25 (Table 3). In the case of cholestan-3-one, the regioselectivity was strict, since only the 25-monohydroxylated derivative was formed by the three enzymes, and the same was observed in the reactions of 4-cholesten-3-one with r*Cci*UPO and *Mro*UPO. However, in the reaction with *Aae*UPO, monohydroxylation at the 4-cholesten-3-one terminal positions (C-26/C-27) also was observed, although as a minor proportion. Interestingly, in the reaction of the diunsaturated cholesta-3,5-dien-7-one, hydroxylation in the steroidal ring also was produced, being especially pronounced in the *Mro*UPO reaction.

The mass spectra of the TMS derivatives of the three 25-monohydroxylated ketones (not shown) showed the above-described characteristic fragment at *m/z* 131 (from C-24–C-25 bond cleavage). No molecular ions for the saturated and monounsaturated ketones were observed, although the molecular masses could be determined from the $[M-15]^+$ fragments (at *m/z* 459 and *m/z* 457, respectively). However, the mass spectrum of the 25-hydroxy-derivative of the diunsaturated ketone showed a molecular ion (*m/z* 470) in addition to the *m/z* 131 and $[M-15]^+$ fragments. Likewise, the 26-hydroxyderivative of 4-cholesten-3-one showed a molecular ion (*m/z* 472) in addition to the *m/z* 131 and $[M-15]^+$ fragments. The diunsaturated cholesta-3,5-dien-7-one yielded the mono- and dihydroxyderivatives, with one hydroxylation at the steroidal ring. The most prominent fragment in the mass spectrum of the monohydroxylated derivative (see Fig. S2A in the supplemental material) corresponded to the molecular ion at *m/z* 470. Other characteristic fragments were observed, but the position of the hydroxyl group in the ring could not be determined. The mass spectrum of the dihydroxylated derivative (see Fig. S2B) showed the characteristic fragment at *m/z* 131. Additionally, a molecular ion (*m/z* 558) and other characteristic fragments were found, but, like in the monohydroxylated derivative, the position of the hydroxyl group in the ring could not be determined.

Steroid hydrocarbon reactions. Cholestane, cholesta-3,5-diene, and pregnane (Fig. 1J to L, respectively) were tested as UPO substrates (Table 1). Cholestane, and especially cholesta-3,5-diene, were transformed by the three peroxygenases, with r*Cci*UPO being the most efficient one. In contrast, pregnane was modified only by *Mro*UPO.

The reaction products of these hydrocarbons are shown in Table 4. Whereas the reaction of cholestane was 100% regioselective at C-25, cholesta-3,5-diene gave several di- and trihydroxylated derivatives at the steroidal ring, in addition to the 25-hydroxy-derivatives (mainly formed by r*Cci*UPO). Among the dihydroxylated derivatives at the ring core, the ones with hydroxylation at C-3 and C-6 are noteworthy (Fig. 2A and B). In these reactions, the saturation of one double bond and displacement of the other one (to C-4) took place. Therefore, the 3,5-diene structure in the substrate was transformed into a 3,6-dihydroxy-4-ene structure. Likewise, the C-3 and C-4 dihydroxylated derivatives lost the double bond at C-3, yielding a 3,4-dihydroxy-5-ene structure. The reaction of pregnane with *Mro*UPO gave several monohydroxylated derivatives at the steroid ring (97% of reaction products), together with a further oxidized derivative (3% 3-ketopregnane) (see Fig. S3 in the supplemental material), although the position of the hydroxyl group could not be determined.

TABLE 2 Abundance of the different oxygenated derivatives identified by GC-MS in the reactions of free sterols with r*Cci*UPO, *Aae*UPO, and *Mro*UPO peroxygenases

Derivative	Abundance (relative %) of derivative with:				
	24-OH	25-OH	26/27-OH	28-OH	26/27-COOH
Cholesterol					
r*Cci*UPO		100			
*Aae*UPO	6	80	9		5
*Mro*UPO		89	6		5
Campesterol					
r*Cci*UPO		85	15		
*Aae*UPO		99	1		
*Mro*UPO		98	2		
Ergosterol					
r*Cci*UPO		100			
*Aae*UPO		100			
*Mro*UPO		100			
Sitosterol					
r*Cci*UPO		52		48	
*Aae*UPO		94		6	
*Mro*UPO		100			
Stigmasterol					
r*Cci*UPO		100			
*Aae*UPO		100			
*Mro*UPO		100			

The mass spectra of the 25-hydroxycholestane and 25-hydroxycholesta-3,5-diene TMS derivatives (not shown) showed the characteristic fragment at *m/z* 131, as well as other characteristic ($[M-15]^+$, $[M-90]^+$, and $[M-90-15]^+$) fragments. The mass spectrum of 3,6-dihydroxycholest-4-ene (Fig. 2A), whose formation is described above, showed a molecular ion (*m/z* 546) and a base peak at *m/z* 403 considered characteristic of the 4-ene-6-hydroxy structure (31) together with other fragments (including $[M-15]^+$,

TABLE 3 Abundance of the different oxygenated derivatives identified by GC-MS in the reactions of steroid ketones with r*Cci*UPO, *Aae*UPO, and *Mro*UPO peroxygenases

Derivative	Abundance (relative %) of derivative with:			
	25-OH	26/27-OH	x-OH	x,25-diOH
Cholestan-3-one				
r*Cci*UPO	100			
*Aae*UPO	100			
*Mro*UPO	100			
4-Cholesten-3-one				
r*Cci*UPO	100			
*Aae*UPO	93	7		
*Mro*UPO	100			
Cholesta-3,5-dien-7-one				
r*Cci*UPO	93			7
*Aae*UPO	87	5	4	4
*Mro*UPO	56		39	5

TABLE 4 Abundance of the different oxygenated derivatives identified by GC-MS in the reactions of steroid hydrocarbons with r*Cci*UPO, *Aae*UPO, and *Mro*UPO peroxygenases

	Abundance (relative %) of derivative with:					
Derivative	25-OH	x-OH	x,25-diOH	3,4-diOH-5-en	3,6-diOH-4-en	3,6,25-triOH-4-en
Cholestane						
r*Cci*UPO	100					
*Aae*UPO	100					
*Mro*UPO	100					
Cholesta-3,5-diene						
r*Cci*UPO	36		14	3	18[a]	29
AaeUPO	3		20	35	31[b]	11
*Mro*UPO			1	36	61[c]	2
Pregnane						
r*Cci*UPO						
*Aae*UPO						
*Mro*UPO		100[d]				

[a] Including 3α,6α-diOH-4-en (14%) and 3β,6β-diOH-4-en (4%).
[b] Including 3α,6α-diOH-4-en (28%) and 3β,6β-diOH-4-en (3%).
[c] Including 3α,6α-diOH-4-en (50%) and 3β,6β-diOH-4-en (11%).
[d] Including 97% hydroxy and 3% keto derivatives (see Fig. S3 in the supplemental material).

$[M-90]^+$, and $[M-15-90]^+$). The mass spectrum of 3,6,25-trihydroxycholest-4-ene (Fig. 2B) showed a molecular ion (*m/z* 634) and the characteristic fragment at *m/z* 131, together with the three additional fragments mentioned above. The mass spectrum of 3,4-dihydroxycholest-4-ene (Fig. 2C) showed a molecular ion (*m/z* 546) and the characteristic fragment at *m/z* 327, together with other fragments (three additional fragments mentioned above plus $[M-90-90]^+$). Finally, the mass spectrum of x,25-dihydroxycholesta-3,5-diene (not shown; where "x" denotes the unknown position of hydroxylation in the ring) showed a molecular ion (*m/z* 544) and the characteristic fragment at *m/z* 131, together with other fragments ($[M-15]^+$ and $[M-90]^+$), but the position of the hydroxyl in the steroid ring could not been determined.

Sterol ester reactions. Cholesteryl acetate, butyrate, and caprylate (Fig. 1M to O, respectively) were tested as UPO substrates (Table 1). The best results were obtained with r*Cci*UPO and cholesteryl acetate, reaching a conversion yield of 34%. Cholesteryl caprylate was not modified by any of the three peroxygenases. In the reactions of sterol esters, the 25-hydroxyderivative was the only product identified. The mass spectra (not shown) showed the characteristic fragment at *m/z* 131 and molecular ions at *m/z* 544 and *m/z* 428 for cholesteryl butyrate and acetate, respectively.

Computational analyses. The molecular structures of eight representative steroids, and that of the *Aae*UPO (PDB entry 2YOR) enzyme, were prepared at the optimal pH for peroxygenase reactions. PELE simulations were performed, providing energy profiles and ligand trajectories. The driving criterion for the simulations was to reduce the distance between the oxygen atom of the peroxygenase compound I and the center of mass of the ligand. From the results of the simulations, we computed the fractions of ligand that entered by the C-25 end and the fractions that entered by the C-3 end. The structures closest to the reactive oxygen then were analyzed as described below. Further detail on energy profiles and interaction maps for each studied steroid in the heme active site are available in the supplemental material (including supplemental computational results and Fig. S4 to S9).

A direct correlation between the percentage of substrate conversion (Table 1) and the percentage of entrance by C-25 was observed (Fig. 3). In the case of cholestane, the fact that it remains 3.6 Å away from the reactive oxygen (see Fig. S7) justifies its reduced reactivity.

A comparison of PELE simulations (binding energy versus distance between substrate C-25 and compound I oxygen) for side-chain hydroxylation of two free sterols and one esterified sterol (cholesterol, sitosterol, and cholesteryl acetate) is shown in Fig. 4, which also includes the main interactions in a representative structure with the ligand at reaction distance from compound I. Cholesterol has the best fraction (82%) of entrance trajectories (Fig. 3). The reason for this is a very hydrophobic heme access channel of peroxygenase, which favors the entrance of the apolar C-25 side. With the side chain in the active site, the molecule then is further stabilized by a hydrogen bond with Glu245 on the surface of the protein (Fig. 4A). Reaction at C-24 and C-26/C-27 also is possible, despite the lower reactivity of secondary and primary carbons compared to that of tertiary C-25, due to the favorable minima with these carbons well positioned for reaction (see Fig. S4 in the supplemental material).

Compared with cholesterol, sitosterol contains an extra ethyl group. This large substituent impedes the access of the substrate to the active site, which is reflected by the lower fraction of structures entering the protein through the C-25 side (39%) compared with cholesterol (Fig. 3). In particular, at the active site the C-28 and C-29 groups clash with Ala77 and Thr192 and reduce considerably the number of structures approaching the heme (Fig. 4B). In addition to C-25, some reaction can be expected at C-28, since the ligand also approaches a favorable distance for the reaction of this additional secondary carbon (data not shown). In spite of its similar structure, the fraction of cholestan-3-one entrance trajectories (49%) also is lower than that found for cholesterol (Fig. 3), and the distance between C-25 and the compound I oxygen is longer (see Fig. S5 in the supplemental material). This is most probably because cholestan-3-one is incapable of hydrogen bonding to Glu245. In the case of cholesta-3,5-dien-7-one, a better approach

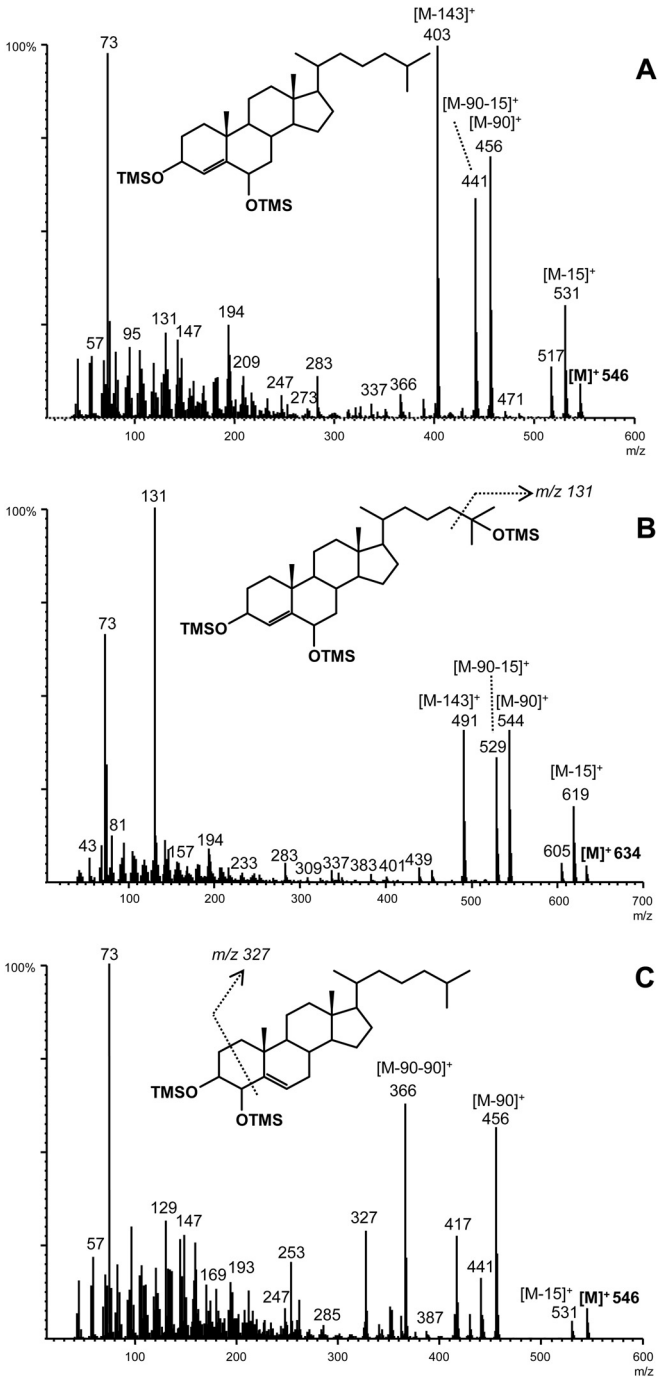

FIG 2 Mass spectra of 3,6-dihydroxycholest-4-ene (A), 3,6,25-trihydroxycholest-4-ene (B), and 3,4-dihydroxycholest-5-ene (C) from peroxygenase reactions, with cholesta-3,5-diene (structure K in Fig. 1) as a TMS derivative.

from the ring side, due to the two double bonds present (see Fig. S6), results in the observed ring hydroxylation.

Cholesteryl acetate has an ester bond at the C-3 hydroxyl, and as in the case of the ketones described above, binding for C-25 oxidation no longer is favored by the hydrogen bond with Glu245 (Fig. 4C), resulting in lower entrance trajectories (35%) than those for cholesterol (Fig. 3); however, an approach from the opposite side did not result in ring hydroxylation. Cholesteryl caprylate has a longer acyl chain than the cholesteryl acetate described above, and (as seen in Fig. S9 in the supplemental material) it does not approach the heme group from either side (the large hydrophobic chains would favor interactions with the protein to avoid solvent exposure).

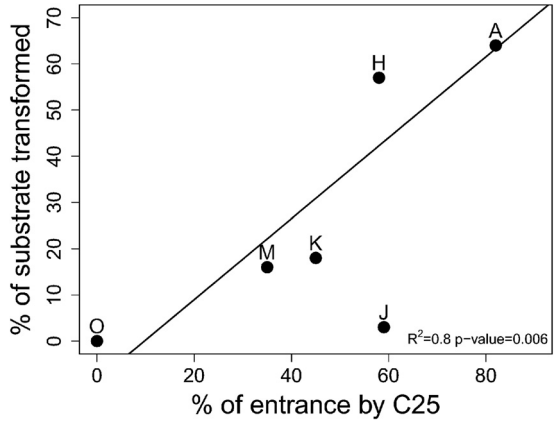

FIG 3 Correlation plot for steroid conversion rate (Table 1) and steroid (side chain) entrance by C-25 to the enzyme active site. Computational results were computed from PELE diffusion simulations (20) of eight selected steroids on the molecular structure of *Aae*UPO (PDB entry 2YOR). For steroid (A to K) identification, see the legend to Fig. 1. Cholestane (compound J) has been removed from the correlation plot (discussed in the text).

Finally, cholesta-3,5-diene has a very interesting reactivity, due to the presence of two double bonds at C-3 and C-5 and the lack of the C-3 hydroxyl mentioned above, that resulted in similar entrance by both C-25 and C-3 positions (Fig. 5A and B, respectively). This explains the fraction of hydroxylated products at the steroid rings, with many of them being additions to its double bonds. In contrast, the bulkier saturated C-5 and C-6 in cholestane (and consequent loss of planarity) impedes a suitable binding of the ligand when it enters by C-25, and a very small number of structures come close enough to the compound I oxygen (see Fig. S7 in the supplemental material), explaining the low reactivity of this compound (cholesterol is converted by 64%, while cholestane is converted by only 3%) (Fig. 3).

DISCUSSION

Despite significant progress in the development of efficient biocatalysts, there is still a great demand for cost-efficient and economical biotechnologies to produce valuable steroids. Most work has been dedicated to steroid modifications catalyzed by whole microbial cells (1). The present work deals with the oxyfunctionalization of steroids using fungal peroxygenases, relatively young representatives of the superfamily of heme-thiolate peroxidases that are characterized by the presence of a cysteine residue as the fifth ligand of the heme iron and their peroxygenase activity (8). Several steroids differing in their structures, including free and esterified sterols and steroid ketones and hydrocarbons, were tested as substrates of peroxygenases from three basidiomycete species. The relationships between the structure of the different substrates, the enzyme reactivity, and the reaction products obtained are discussed below. A combined experimental and computational approach shows that there is not a unique factor that determines the hydroxylation profile; instead, it is a result of the sum of many structural factors, concerning both the steroid mol-

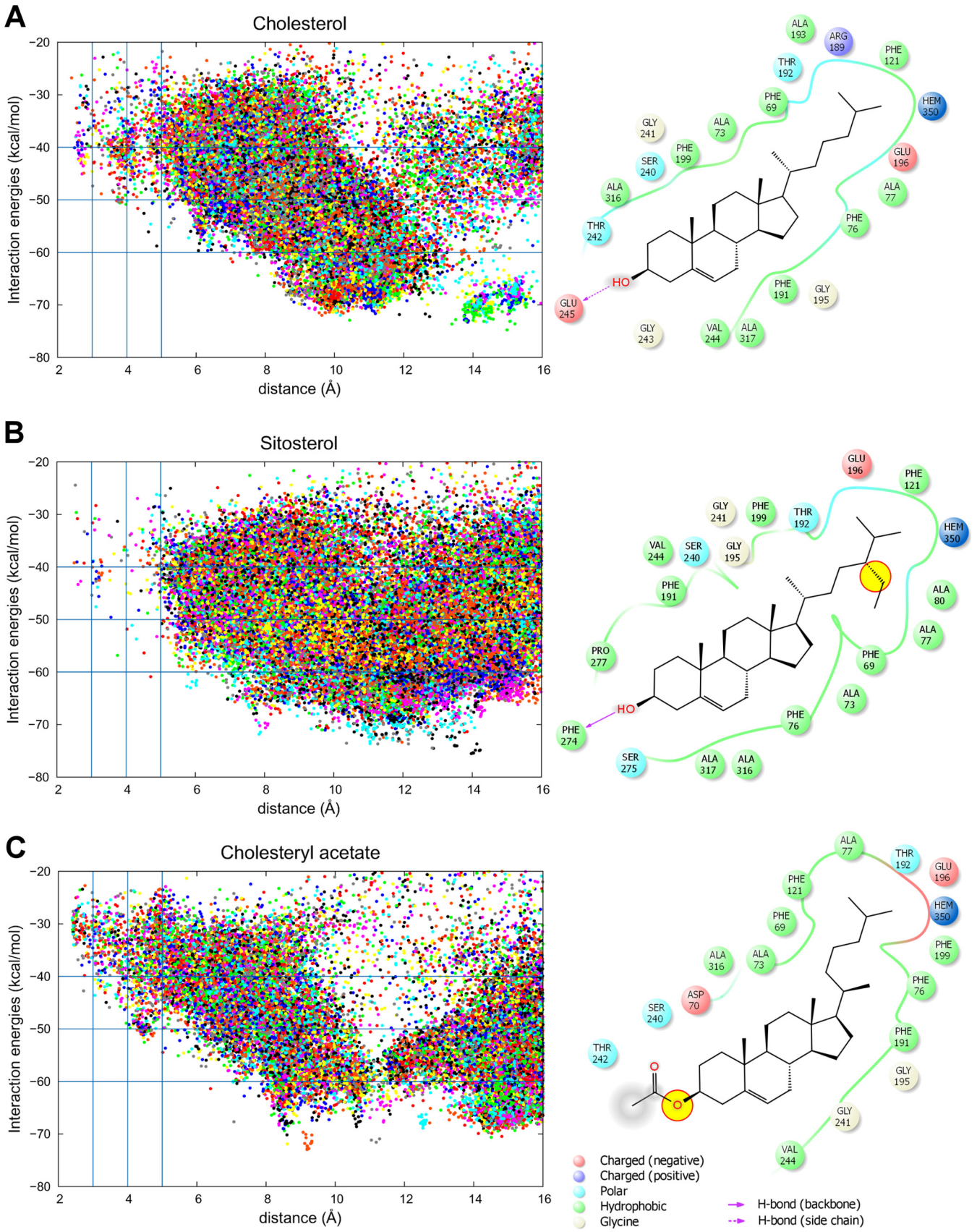

FIG 4 Results from PELE (20) simulations for cholesterol (A), sitosterol (B), and cholesteryl acetate (C) diffusion at the active site of the *Aae*UPO, including (left) plots of the energy profile versus the distance between the steroid H25 and the oxygen atom in enzyme compound I and (right) main interactions between the substrate and the enzyme in a representative structure for each of the three steroids analyzed. The yellow circles identify structural differences relative to the structure of cholesterol.

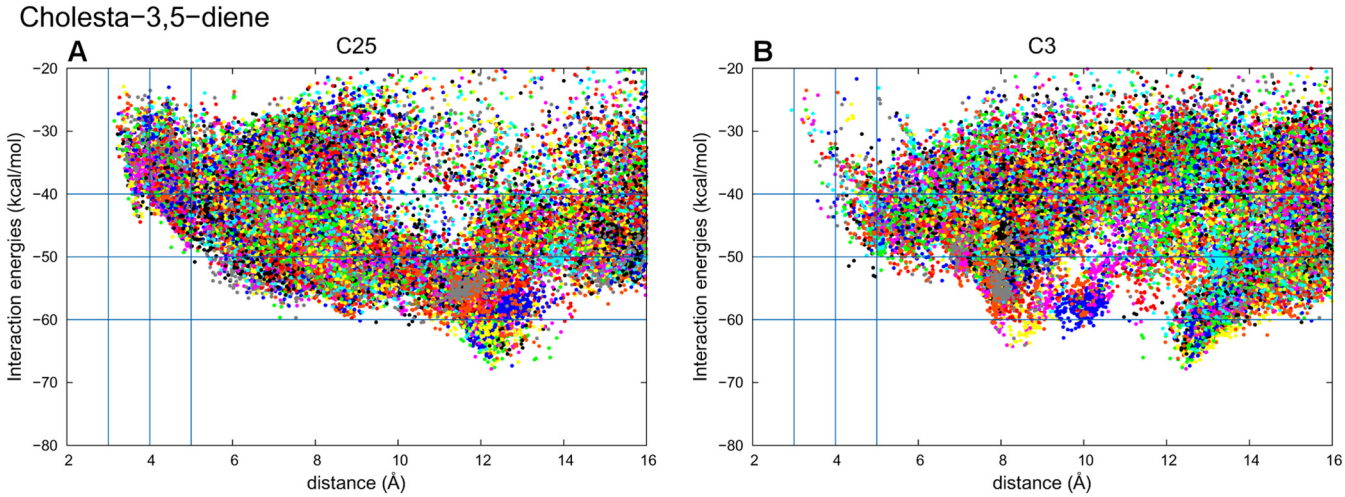

FIG 5 Results from PELE (20) simulations for cholesta-3,5-diene diffusion at the active site with C-25 (A) or C-3 (B) approaching the heme cofactor of the *Aae*UPO.

ecule and the enzyme active site. These include the polar/apolar character of C-3/C-7 ring groups, the presence of double bonds in the steroidal rings, and the length and character of the alkyl C-17 chain, which affect the ligand entrance ratio on the C-25 side.

Relationships between steroid structure and conversion yield. The influence of the C-17 alkyl chain, oxidation/unsaturation of the rings, and esterification of the C-3 hydroxyl group on the steroid conversions is discussed below.

(i) Alkyl chain at C-17. The influence of the steroid alkyl side chain substitution and unsaturation was shown by the different extents of transformation obtained for C_{27}, C_{28}, and C_{29} sterols. The C_{27} cholesterol was completely transformed by r*Cci*UPO, while the other sterols were transformed to a lesser extent by this and the two other peroxygenases. The presence of a methyl or ethyl group at C-24 makes it progressively more difficult to hydroxylate campesterol and sitosterol, as illustrated in Fig. 6. Moreover, the double bond at C-22, in addition to the methyl or ethyl group at C-24, made ergosterol and stigmasterol more difficult to be hydroxylated (by the three peroxygenases) than the above-described campesterol and sitosterol. The influence of a shorter side chain was shown by comparing the hydroxylation of pregnane (with an ethyl group at C-17) and other steroid hydrocarbons (e.g., cholestane). The presence of a two-carbon (instead of eight-carbon) alkyl chain prevents hydroxylation by r*Cci*UPO and *Aae*UPO and, in contrast, promotes hydroxylation by *Mro*UPO, which takes place in the steroidal ring (not in the side chain). Finally, the absence of an alkyl chain at C-17, like in testosterone (having instead a hydroxyl group), completely prevents its hydroxylation by the three fungal peroxygenases (compared with up to 100% conversion of 4-cholesten-3-one).

The good conversion produced in the reactions of peroxygenases with cholesterol and the differences observed in the conversion of sterols with different alkyl chain sizes, like sitosterol, are explained by computational results. In general terms, the polarity of the substituent group at C-3 has a positive correlation with the ligand rate entrance by the C-25 side. This is due to the hydrophobic character of the protein access channel to the heme that contains numerous phenylalanine residues. Moreover, the presence of a hydroxyl group in C-3 (of cholesterol and other sterols) increases the ligand rate entrance by the C-25 side and stabilizes the ligand in a suitable catalytic position (a good catalytic position is assumed when the distance between the hydrogen in C-25 and the compound I oxygen is around 2.4 Å) due to a hydrogen bond with Glu245. These two factors correlate perfectly with the high activity shown for cholesterol. However, although sitosterol also has a hydroxyl group in C-3, it is not able to access the heme site by the C-25 end in the same way as cholesterol due to the bulkier alkyl chain in C-17 that clashes with residues in the heme access channel (namely, Thr192, Ala77, Phe69, Phe121, and Phe199).

(ii) Oxidation/unsaturation degree of the rings. Steroids differing in the oxidation state of the ring were tested, including steroid hydrocarbons, sterols, and steroid ketones. Whereas r*Cci*UPO completely converted both cholesterol and 4-cholesten-3-one, *Aae*UPO and *Mro*UPO oxidized the ketone with lower efficiency. The contrary was reported for P450s (e.g., CYP27A1), which hydroxylated steroids with a 3-oxo-Δ^4 structure at a much higher rate than those with a 3β-hydroxy-Δ^5 structure (32). Therefore, the structural differences between 4-cholesten-3-one and cholesterol, which are the planarity of the sterol A-ring and the electronic properties resulting from a keto versus hydroxyl substituent at C-3, seemingly affect the peroxygenase activity. The computational results revealed that the polar character of the hydroxyl and oxo groups in the sterols and steroid ketones affects in a positive way the ligand entrance rate by C-25, which correlates with the high activity that these compounds show compared with the corresponding steroid hydrocarbons.

On the other hand, although differences were observed between the three peroxygenases, the presence and number of double bonds in the rings of steroid hydrocarbons and ketones significantly increases their hydroxylation degree. This is illustrated in Fig. 7, where better *Aae*UPO conversion of cholesta-3,5-diene and cholesta-3,5-dien-7-one, compared with that of the corresponding saturated molecules (cholestane and cholestan-3-one), is shown. The C-25 side entrance and the placement of the steroid hydrocarbons in a proper catalytic position are determined by the presence or absence of double bonds. These reduce the volume of the steroid ring, facilitating its entrance in the active site, and provide proper curvature to the substrate for an optimal approach

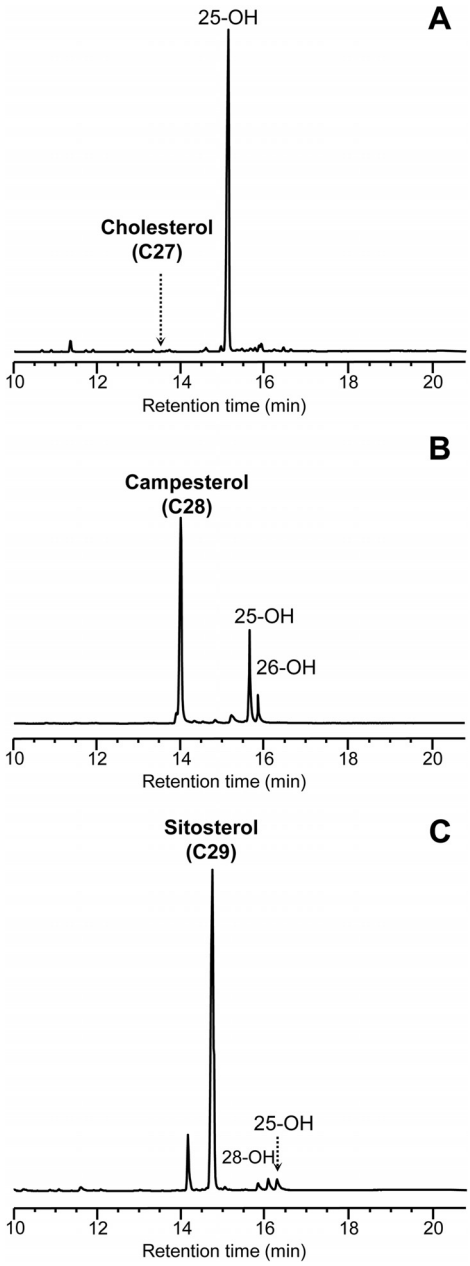

FIG 6 GC-MS analysis of the r*Cci*UPO reaction (at 60 min) with cholesterol (A), campesterol (B), and sitosterol (C) (depicted in Fig. 1) showing the remaining substrates and the monohydroxylated derivatives at C-25, C-26, and C-28 of the side chain.

to the heme. Therefore, both the apolar nature of the two extremes of the molecule and the presence of double bonds in cholesta-3,5-diene facilitate access to the heme from both sides, C-3 and C-25, and its correct placement for reaction. However, neither the substrate entrance nor its placement in the active site are as suitable as they are in sterols and steroid ketones. In the case of cholestane, the entrance to the heme site is hampered by the larger sp3 groups at C-3, C-4, C-6, and C-7. This can be better observed by comparing the energy profiles of this compound (see Fig. S7 in the supplemental material) to those of cholesta-3,5-diene (see Fig. S8) and observing the very different occupation of the binding site. In addition, the higher reactivity of alkenes than alkanes leads to addition of hydroxyl groups to the double bonds in the steroidal rings in cholesta-3,5-diene, which is not observed in cholestane. Concerning the two ketones compared in Fig. 7C and D, although both have a similar ratio for C-25 entrance, cholestan-3-one can be hydroxylated at only C-25, while cholesta-3,5-dien-7-one shows some additional hydroxylation due to the higher reactivity of the alkenes mentioned above. Moreover, as in the case of the steroid hydrocarbons, the two double bonds in the steroid ketone ring will facilitate the entrance and proper positioning of the substrate at the peroxygenase active site.

Due to the above-described effects, although the conversion rates of cholestan-3-one are lower than those of cholesterol (the best steroid substrate of the basidiomycete peroxygenases), they are increased by the presence of double bonds in the steroid ring, and cholestan-3,5-dien-7-one hydroxylation rates are in the same order of those obtained for cholesterol.

(**iii**) **Esterified hydroxyl group at C-3.** With the aim of investigating whether the hydroxyl group at C-3, in free form, is necessary for maximal peroxygenase activity, three esters of cholesterol with organic acids of different chain lengths were assayed as substrates. The experimental results revealed that the presence of an esterifying group hampers substrate conversion, and that this effect is directly correlated with increasing chain length of the fatty acid. In sterol esters, hydroxylation (at C-25) only of the side chain of the sterol was observed and not at the acyl moiety, despite *Aae*UPO and r*Cci*UPO being found to efficiently hydroxylate fatty acids (11, 18).

The computational analyses revealed that in the sterol esters, the C-25 entrance rate is decreased with respect to cholesterol due to the presence of hydrophobic alkyl chains at the ester site. In the case of cholesteryl caprylate, which is not transformed by any of the peroxygenases, the long unsubstituted hydrocarbon chain tends to "anchor" the substrate away from the heme site by interacting with different groups on the protein surface. Since both ends are hydrophobic, interactions with the protein minimize the solvent exposure but restrain the ligand from reaching the heme, which explains the lack of activity for this compound.

Relationships between steroid structure and regioselectivity. In general, the reactions of the three fungal peroxygenases with the different steroids proceed with remarkable regioselectivity and result in the formation of the 25-hydroxyderivatives as the main products. The complete conversion of cholesterol by r*Cci*UPO to produce 25-hydroxycholesterol is noteworthy, since this compound is widely used, displaying an array of pharmacological actions *in vitro* and in cell-based systems (33), as discussed below. Different alkyl chains at C-17 seemingly do not influence the regioselectivity in *Aae*UPO and *Mro*UPO reactions (see below) but affect that of r*Cci*UPO, since cholesterol is C-25 hydroxylated with a strict (100%) regioselectivity, whereas for campesterol and sitosterol, hydroxylation at terminal C-26/C-27 (15%) and subterminal C-28 (48%), respectively, also was observed. On the other hand, the double bond at C-22 in ergosterol and stigmasterol seemingly influences the strict regioselectivity of the hydroxylation at C-25. Minor hydroxylation at the terminal positions of the steroid branched side chain by *Aae*UPO and *Mro*UPO also leads in some cases (e.g., cholesterol) to formation of the C-26/C-27-carboxylated derivatives, in addition to the C-26/C-27-hydroxylated ones. This is because of the further oxidation (successive hydroxylation and dehydration reactions) of the monohydroxylated prod-

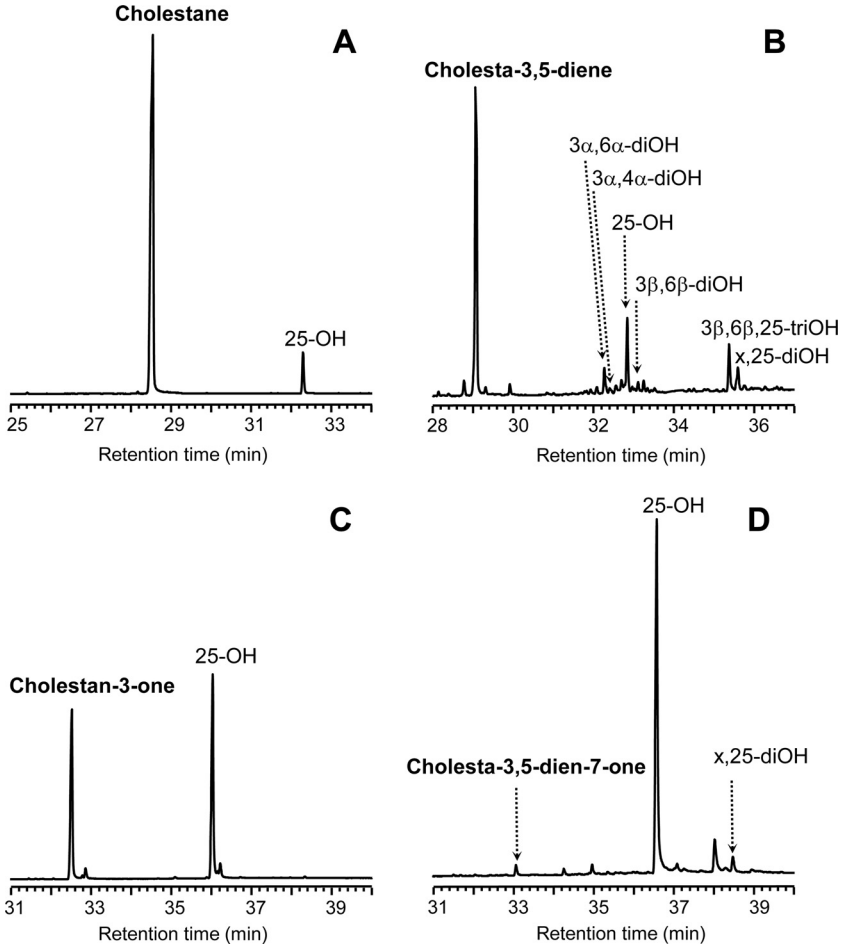

FIG 7 GC-MS analysis of the r*Cci*UPO reaction (at 60 min) with cholestane (A), cholesta-3,5-diene (B), cholestan-3-one (C), and cholesta-3,5-diene-7-one (D) (depicted in Fig. 1) showing the remaining substrates and the mono-, di-, and trihydroxylated derivatives included in Table 4 (x denotes the unknown position of hydroxylation in the ring).

ucts, as previously demonstrated in ^{18}O-labeling oxygenation studies with *Aae*UPO and $H_2{}^{18}O_2$ (11).

Hydroxylation at positions other than C-25 occurs in cases that show a high (energetically favorable) occupation of binding positions near any of these centers, as demonstrated for *Aae*UPO by computational studies. In particular, the case of cholesterol hydroxylation at C-24 is due to interactions between the substrate and the protein that include a local minima for C-24, which is slightly more favorable than that for C-25. Hydroxylation at C-25 (tertiary C-H bond) is electronically preferred by its lower C-H bond strength compared with that of the secondary and primary C-H bonds (34). In contrast, steric constraints rather than the differential electronic properties of the C-H bonds have been reported to govern the regioselectivity of the reaction of steroids (cholesterol and 4-cholesten-3-one) with P450s (CYP125A1) where terminal oxidation was preferred (35).

Interestingly, in addition to hydroxylation at the side chain, some hydroxylated derivatives at the steroid core are formed when oxygen groups are lacking at C-3, such as in cholesta-3,5-dione, cholesta-3,5-diene, or pregnane. Indeed, the presence of a hydroxyl or oxo group at this position seems to prevent the hydroxylation of the steroidal core. On the other hand, the presence of two conjugated double bonds in the ring seems to favor the hydroxylation at the steroidal core, especially by *Aae*UPO and *Mro*UPO, as evidenced in the reaction of cholesta-3,5-diene yielding 3,6-dihydroxycholest-4-ene and 3,4-dihydroxycholest-5-ene, as mentioned above. The mechanism of this double (at C-3 and C-6 or at C-3 and C-4) hydroxylation implies the displacement of one of the cholesta-3,5-diene double bonds to the intermediate (C-4 or C-5) position and the saturation of the other.

Significance of side-chain versus ring hydroxylation. It has been shown that the reactions of the peroxygenases from the three different basidiomycetes occurred generally with noteworthy regioselectivity, and hydroxylation at the side chain over the steroidal ring was preferred, with the 25-hydroxyderivatives predominating. From a biochemical point of view, side-chain and steroid nucleus oxidation have been confirmed to be independent processes, at least in some microorganisms (1). Side-chain hydroxylation is usually a prestep in side-chain degradation in most microbial systems that oxidize steroids. The initial step of the side-chain oxidation of sterols (and other C_{27} steroids) is hydroxylation at C-26 or C-27, followed by a complex sequence of reactions involving different enzymes (some of them still unidentified) that produce the elimination of side chain at C-17 and then steroidal nucleus oxidation. However, further oxidative degradation on the C-17 side chain may not occur when hydroxylation is

produced at C-25 (instead of C-26 or C-27). This has been observed using 25-hydroxylated cholesterol as the substrate (36), concluding that C-25 hydroxylation must be a distinct reaction from that of the usual cholesterol side chain degradation pathway. Indeed, the authors do not consider that steroid metabolism is a specific function of UPOs, not as much as it is the oxidation of alkanes, alkenes, ethers, or aromatics. Rather, UPOs represent a catalytic system ("extracellular liver") that, irrespective of a particular structure, can nonspecifically oxidize diverse compounds emerging in the fungus microenvironment. In this context, unspecific detoxification surely is more important than specific degradation.

Interestingly, a previously unrecognized biological (antiviral) role for 25-hydroxycholesterol, which is selectively formed by the r*Cci*UPO as discussed above, has been highlighted recently (37). Indeed, that study revealed 25-hydroxycholesterol as the only oxysterol notably upregulated following macrophage infection or activation by interferons. This antiviral effect is specific to 25-hydroxycholesterol, because other related (enzymatically generated) oxysterols, such as 19-hydroxychoesterol and 7α-hydroxycholesterol, fail to repress viral infection. 25-Hydroxycholesterol has been reported to have a high potency to inhibit a broad spectrum of viruses from high to low physiological concentrations depending on lipid conditions and virus-host cell system. Likewise, other recent studies also revealed 25-hydroxycholesterol as a potential antiviral therapeutic (38). Independent of its known regulatory effect on metabolism, 25-hydroxycholesterol impairs viral entry at the virus-cell fusion step by inducing cellular membrane changes. Because 25-hydroxycholesterol can permeate through membranes, it likely modifies cellular membranes to exert its antiviral effect. Moreover, in addition to interfering with viral entry and replication, 25-hydroxycholesterol also amplifies the activation of immune cells and increases the production of immune mediators (39).

Final remarks. The first crystal structure of a fungal peroxygenase (23), from the basidiomycete *A. aegerita* (*Aae*UPO), was used in the computational simulations included in the present study. The availability of more peroxygenase crystal structures, including those from *C. cinerea* and *M. rotula*, will provide the opportunity to correlate the different regioselectivities in steroid oxygenation described here with the architecture of the active site and other structural features. Such information will permit us to engineer these self-sufficient monooxygenases (whose activation depends on a peroxide source) as new and robust industrial biocatalysts for the pharmaceutical and fine-chemical sectors.

In conclusion, in the present work, the ability of three different fungal peroxygenases to catalyze the regioselective hydroxylation of a variety of steroids is shown for the first time. Generally, hydroxylation at the side chain over the steroid ring was preferred, with 25-hydroxyderivatives being the main products formed. It has been observed that some structural features of the steroid substrates, such as the presence and length of the alkyl chain at C-17 and the presence of oxygen groups and/or conjugated double bonds in the steroid ring system, influence substrate conversion and guide the regioselectivity of the reactions. A better understanding of the mechanistic aspects of hydroxylation in combination with the development of suitable biocatalysts would be the basis for efficient steroid hydroxylation bioprocesses using new enzymes with self-sufficient mono(per)oxygenase activities.

ACKNOWLEDGMENTS

This study was supported by the INDOX (KBBE-2013-7-613549), PEROXICATS (KBBE-2010-4-265397), and PELE (ERC-2009-Adg 25027) EU projects.

We have no conflicts of interest to declare.

REFERENCES

1. **Donova MV, Egorova OV.** 2012. Microbial steroid transformations: current state and prospects. Appl Microbiol Biotechnol **94:**1423–1447. http://dx.doi.org/10.1007/s00253-012-4078-0.
2. **Beneventi E, Ottolina G, Carrea G, Panzeri W, Fronza G, Lau PCK.** 2009. Enzymatic Baeyer-Villiger oxidation of steroids with cyclopentadecanone monooxygenase. J Mol Catal B Enzym **58:**164–168. http://dx.doi.org/10.1016/j.molcatb.2008.12.009.
3. **Ortiz de Montellano PR.** 2005. Cytochrome P450: structure, mechanism, and biochemistry. Kluwer Academic/Plenum, New York, NY.
4. **Urlacher VB, Girhard M.** 2012. Cytochrome P450 monooxygenases: an update on perspectives for synthetic application. Trends Biotechnol **30:**26–36. http://dx.doi.org/10.1016/j.tibtech.2011.06.012.
5. **van Beilen JB, Funhoff EG.** 2005. Expanding the alkane oxygenase toolbox: new enzymes and applications. Curr Opin Biotechnol **16:**308–314. http://dx.doi.org/10.1016/j.copbio.2005.04.005.
6. **Li H.** 2001. Cytochrome P450, p 267–282. *In* Messerschmidt A, Huber R, Poulos TL, Wieghardt K (ed), Handbook of metalloproteins, vol 1. Wiley, Chichester, United Kingdom.
7. **Ullrich R, Nuske J, Scheibner K, Spantzel J, Hofrichter M.** 2004. Novel haloperoxidase from the agaric basidiomycete *Agrocybe aegerita* oxidizes aryl alcohols and aldehydes. Appl Environ Microbiol **70:**4575–4581. http://dx.doi.org/10.1128/AEM.70.8.4575-4581.2004.
8. **Hofrichter M, Ullrich R.** 2014. Oxidations catalyzed by fungal peroxygenases. Curr Opin Chem Biol **19:**116–125. http://dx.doi.org/10.1016/j.cbpa.2014.01.015.
9. **Bernhardt R.** 2006. Cytochromes P450 as versatile biocatalysts. J Biotechnol **124:**128–145. http://dx.doi.org/10.1016/j.jbiotec.2006.01.026.
10. **Hofrichter M, Ullrich R, Pecyna MJ, Liers C, Lundell T.** 2010. New and classic families of secreted fungal heme peroxidases. Appl Microbiol Biotechnol **87:**871–897. http://dx.doi.org/10.1007/s00253-010-2633-0.
11. **Gutiérrez A, Babot ED, Ullrich R, Hofrichter M, Martínez AT, del Río JC.** 2011. Regioselective oxygenation of fatty acids, fatty alcohols and other aliphatic compounds by a basidiomycete heme-thiolate peroxidase. Arch Biochem Biophys **514:**33–43. http://dx.doi.org/10.1016/j.abb.2011.08.001.
12. **Peter S, Kinne M, Wang X, Ullrich R, Kayser G, Groves JT, Hofrichter M.** 2011. Selective hydroxylation of alkanes by an extracellular fungal peroxygenase. FEBS J **278:**3667–3675. http://dx.doi.org/10.1111/j.1742-4658.2011.08285.x.
13. **Anh DH, Ullrich R, Benndorf D, Svatos A, Muck A, Hofrichter M.** 2007. The coprophilous mushroom *Coprinus radians* secretes a haloperoxidase that catalyzes aromatic peroxygenation. Appl Environ Microbiol **73:**5477–5485. http://dx.doi.org/10.1128/AEM.00026-07.
14. **Gröbe G, Ullrich M, Pecyna M, Kapturska D, Friedrich S, Hofrichter M, Scheibner K.** 2011. High-yield production of aromatic peroxygenase by the agaric fungus *Marasmius rotula*. AMB Express **1:**31–42. http://dx.doi.org/10.1186/2191-0855-1-31.
15. **Pecyna MJ, Ullrich R, Bittner B, Clemens A, Scheibner K, Schubert R, Hofrichter M.** 2009. Molecular characterization of aromatic peroxygenase from *Agrocybe aegerita*. Appl Microbiol Biotechnol **84:**885–897. http://dx.doi.org/10.1007/s00253-009-2000-1.
16. **Floudas D, Binder M, Riley R, Barry K, Blanchette RA, Henrissat B, Martínez AT, Otillar R, Spatafora JW, Yadav JS, Aerts A, Benoit I, Boyd A, Carlson A, Copeland A, Coutinho PM, de Vries RP, Ferreira P, Findley K, Foster B, Gaskell J, Glotzer D, Górecki P, Heitman J, Hesse C, Hori C, Igarashi K, Jurgens JA, Kallen N, Kersten P, Kohler A, Kües U, Kumar TKA, Kuo A, LaButti K, Larrondo LF, Lindquist E, Ling A, Lombard V, Lucas S, Lundell T, Martin R, McLaughlin DJ, Morgenstern I, Morin E, Murat C, Nolan M, Ohm RA, Patyshakuliyeva A, Rokas A, Ruiz-Dueñas FJ, Sabat G, Salamov A, Samejima M, Schmutz J, Slot JC, St John F, Stenlid J, Sun H, Sun S, Syed K, Tsang A, Wiebenga A, Young D, Pisabarro A, Eastwood DC, Martin F, Cullen D, Grigoriev IV, Hibbett DS.** 2012. The Paleozoic origin of enzymatic lignin decomposition reconstructed from 31 fungal genomes. Science **336:**1715–1719. http://dx.doi.org/10.1126/science.1221748.

17. **Stajich JE, Wilke SK, Ahren D, Au CH, Birren BW, Borodovsky M, Burns C, Canback B, Casselton LA, Cheng CK, Deng JX, Dietrich FS, Fargo DC, Farman ML, Gathman AC, Goldberg J, Guigo R, Hoegger PJ, Hooker JB, Huggins A, James TY, Kamada T, Kilaru S, Kodira C, Kues U, Kupfert D, Kwan HS, Lomsadze A, Li WX, Lilly WW, Ma LJ, Mackey AJ, Manning G, Martin F, Muraguchi H, Natvig DO, Palmerini H, Ramesh MA, Rehmeyer CJ, Roe BA, Shenoy N, Stanke M, Ter Hovhannisyan V, Tunlid A, Velagapudi R, Vision TJ, Zeng QD, Zolan ME, Pukkila PJ.** 2010. Insights into evolution of multicellular fungi from the assembled chromosomes of the mushroom *Coprinopsis cinerea* (*Coprinus cinereus*). Proc Natl Acad Sci U S A **107:**11889–11894. http://dx.doi.org/10.1073/pnas.1003391107.
18. **Babot ED, del Río JC, Kalum L, Martínez AT, Gutiérrez A.** 2013. Oxyfunctionalization of aliphatic compounds by a recombinant peroxygenase from *Coprinopsis cinerea*. Biotechnol Bioeng **110:**2332. http://dx.doi.org/10.1002/bit.24904.
19. **Cossins BP, Hosseini A, Guallar V.** 2012. Exploration of protein conformational change with PELE and meta-dynamics. J Chem Theory Comput **8:**959–965. http://dx.doi.org/10.1021/ct200675g.
20. **Borrelli KW, Vitalis A, Alcantara R, Guallar V.** 2005. PELE: protein energy landscape exploration. A novel Monte Carlo based technique. J Chem Theory Comput 1:1304–1311.
21. **Ullrich R, Liers C, Schimpke S, Hofrichter M.** 2009. Purification of homogeneous forms of fungal peroxygenase. Biotechnol J **4:**1619–1626. http://dx.doi.org/10.1002/biot.200900076.
22. **Gutiérrez A, del Río JC, González-Vila FJ, Martín F.** 1998. Analysis of lipophilic extractives from wood and pitch deposits by solid-phase extraction and gas chromatography. J Chromatogr **823:**449–455. http://dx.doi.org/10.1016/S0021-9673(98)00356-2.
23. **Piontek K, Strittmatter E, Ullrich R, Grobe G, Pecyna MJ, Kluge M, Scheibner K, Hofrichter M, Plattner DA.** 2013. Structural basis of substrate conversion in a new aromatic peroxygenase: cytochrome P450 functionality with benefits. J Biol Chem **288:**34767–34776. http://dx.doi.org/10.1074/jbc.M113.514521.
24. **Sastry GM, Adzhigirey M, Day T, Annabhimoju R, Sherman W.** 2013. Protein and ligand preparation: parameters, protocols, and influence on virtual screening enrichments. J Comput Aided Mol Des **27:**221–234. http://dx.doi.org/10.1007/s10822-013-9644-8.
25. **Anandakrishnan R, Aguilar B, Onufriev AV.** 2012. H++3.0: automating pK prediction and the preparation of biomolecular structures for atomistic molecular modeling and simulations. Nucleic Acids Res **40:**W537–W541. http://dx.doi.org/10.1093/nar/gks375.
26. **Kaminski GA, Friesner RA, Tirado-Rives J, Jorgensen WL.** 2001. Evaluation and reparametrization of the OPLS-AA force field for proteins via comparison with accurate quantum chemical calculations on peptides. J Phys Chem B **105:**6474–6487. http://dx.doi.org/10.1021/jp003919d.
27. **Bashford D, Case DA.** 2000. Generalized born models of macromolecular solvation effects. Annu Rev Phys Chem **51:**129–152. http://dx.doi.org/10.1146/annurev.physchem.51.1.129.
28. **Linde D, Pogni R, Cañellas M, Lucas F, Guallar V, Baratto MC, Sinicropi A, Sáez-Jiménez V, Coscolín C, Romero A, Medrano FJ, Ruiz-Dueñas FJ, Martínez AT.** 2014. Catalytic surface radical in dye-decolorizing peroxidase: a computational, spectroscopic and directed mutagenesis study. Biochem J **50:**5096–5107. http://dx.doi.org/10.1042/BJ20141211.
29. **Hernández-Ortega A, Lucas F, Ferreira P, Medina M, Guallar V, Martínez AT.** 2011. Modulating O2 reactivity in a fungal flavoenzyme: involvement of aryl-alcohol oxidase Phe-501 contiguous to catalytic histidine. J Biol Chem **286:**41105–41114. http://dx.doi.org/10.1074/jbc.M111.282467.
30. **Lucas MF, Guallar V.** 2012. An atomistic view on human hemoglobin carbon monoxide migration processes. Biophys J **102:**887–896. http://dx.doi.org/10.1016/j.bpj.2012.01.011.
31. **Brooks CJW, Henderson W, Steel G.** 1973. Use of trimethylsilyl ethers in characterization of natural sterols and steroid diols by gas chromatography mass spectrometry. Biochim Biophys Acta **296:**431–445. http://dx.doi.org/10.1016/0005-2760(73)90101-X.
32. **Norlin M, von Bahr S, Bjorkhem I, Wikvall K.** 2003. On the substrate specificity of human CYP27A1: implications for bile acid and cholestanol formation. J Lipid Res **44:**1515–1522. http://dx.doi.org/10.1194/jlr.M300047-JLR200.
33. **Diczfalusy U.** 2013. On the formation and possible biological role of 25-hydroxycholesterol. Biochimie **95:**455–460. http://dx.doi.org/10.1016/j.biochi.2012.06.016.
34. **Johnston JB, Ouellet H, Podust LM, Ortiz de Montellano PR.** 2011. Structural control of cytochrome P450-catalyzed ω-hydroxylation. Arch Biochem Biophys **507:**86–94. http://dx.doi.org/10.1016/j.abb.2010.08.011.
35. **Ouellet H, Guan SH, Johnston JB, Chow ED, Kells PM, Burlingame AL, Cox JS, Podust LM, de Montellano PR.** 2010. *Mycobacterium tuberculosis* CYP125A1, a steroid C27 monooxygenase that detoxifies intracellularly generated cholest-4-en-3-one. Mol Microbiol **77:**730–742. http://dx.doi.org/10.1111/j.1365-2958.2010.07243.x.
36. **Wang KC, Wang PH, Lee SS.** 1997. Microbial transformation of protopanaxadiol and protopanaxatriol derivatives with *Mycobacterium* sp. (NRRL B-3805). J Nat Prod **60:**1236–1241. http://dx.doi.org/10.1021/np970331y.
37. **Blanc M, Hsieh WY, Robertson KA, Kropp KA, Forster T, Shui GH, Lacaze P, Watterson S, Griffiths SJ, Spann NJ, Meljon A, Talbot S, Krishnan K, Covey DF, Wenk MR, Craigon M, Ruzsics Z, Haas J, Angulo A, Griffiths WJ, Glass CK, Wang YQ, Ghazal P.** 2013. The transcription factor STAT-1 couples macrophage synthesis of 25-hydroxycholesterol to the interferon antiviral response. Immunity **38:**106–118. http://dx.doi.org/10.1016/j.immuni.2012.11.004.
38. **Liu SY, Aliyari R, Chikere K, Li GM, Marsden MD, Smith JK, Pernet O, Guo HT, Nusbaum R, Zack JA, Freiberg AN, Su LS, Lee B, Cheng GH.** 2013. Interferon-inducible cholesterol-25-hydroxylase broadly inhibits viral entry by production of 25-hydroxycholesterol. Immunity **38:**92–105. http://dx.doi.org/10.1016/j.immuni.2012.11.005.
39. **Gold ES, Diercks AH, Podolsky I, Podyminogin RL, Askovich PS, Treuting PM, Aderem A.** 2014. 25-Hydroxycholesterol acts as an amplifier of inflammatory signaling. Proc Natl Acad Sci U S A **111:**10666–10671. http://dx.doi.org/10.1073/pnas.1404271111.
40. **Schnorr KM, Ullrich R, Scheibner K, Kluge MG, Hofrichter M.** October 2008. Fungal peroxygenases and methods of application. World Intellectual Property Organization patent WO/2008/119780.

Supplemental Material

Steroid hydroxylation by basidiomycete peroxygenases: A combined experimental and computational study

Esteban D. Babot,[a] José C. del Río,[a] Marina Cañellas,[b,c] Ferran Sancho,[b,c] Fátima Lucas,[b] Víctor Guallar,[b,d] L. Kalum,[e] Henrik Lund,[e] Glenn Gröbe,[f] Katrin Scheibner,[f] René Ullrich,[g] Martin Hofrichter,[g] Angel T. Martínez[h] and Ana Gutiérrez[a*]

[a]Instituto de Recursos Naturales y Agrobiología de Sevilla, CSIC, Reina Mercedes 10, E-41012 Seville, Spain

[b]Joint BSC-CRG-IRB Research Program in Computational Biology, Barcelona Supercomputing Center, Jordi Girona 29, E-08034 Barcelona, Spain,

[c]Anaxomics Biotech, Balmes 89, E-08008 Barcelona, Spain

[d]ICREA, Passeig Lluís Companys 23, E-08010 Barcelona, Spain

[e]Novozymes A/S, Krogshoejvej 36, 2880 Bagsvaerd, Denmark

[f]JenaBios GmbH, Orlaweg 2, 00743 Jena, Germany

[g]TU Dresden, Department of Bio- and Environmental Sciences, Markt 23, 02763 Zittau, Germany

[h]Centro de Investigaciones Biológicas, CSIC, Ramiro de Maeztu 9, E-28040 Madrid, Spain

The Supplemental Material include Supplemental Computational Results, and Supplemental Figures showing mass spectrum of 25-hydroxycholesterol (**Fig. S1**), mass spectra of x-hydroxycholesta-3,5-dien-7-one and 25,x-dihydroxycholesta-3,5-dien-7-one (**Fig. S2**), and chromatogram of the pregnane reaction (**Fig. S3**); together with PELE simulations for cholesterol (**Fig. S4**), cholestan-3-one (**Fig. S5**), cholesta-3,5-dien-7-one (**Fig. S6**), cholestane (**Fig. S7**), cholesta-3,4-diene (**Fig. S8**) and cholesteryl caprylate (**Fig. S9**).

Supplemental Computational Results

Free and esterified sterols

Cholesterol (compound A in **Fig. 1**) has the best fraction of trajectories entering by the C25 side (82%) (**Fig. 3**). The reason for this is a hydrophobic entrance to the heme side which favors the entrance by the apolar side of the ligand. Then in the active site the molecule is further stabilized by a hydrogen bond with Glu245 on the surface of the protein (**Fig. 4A**). Reactions at C24 (**Fig. S4A**) and C26/C27 (**Fig. S4C** and **D**) are possible despite the less favorable breaking of secondary and primary C-H bonds due to the presence of minima with these hydrogens well positioned for reaction with compound I. In particular C24 approaches the heme with a more favorable interaction energy than C25.

Sitosterol (compound D in **Fig. 1**) contains an extra ethyl group at C24. This large substituent impedes the entrance of the substrate in the active site, which is reflected by the lower fraction of structures entering the protein through C25 side (39% opposed to 82% for compound A) (**Fig. 3**). In particular, at the active site the C28 and C29 groups clash with Ala77 and Thr192 which reduces considerably the number of structures capable of approaching the heme at a reactive distance (**Fig. 4B**). Some reaction can nevertheless be expected at C28 due to the fact that simulations show that the ligand approaches the heme to a favorable distance for reaction at this secondary carbon.

* Address correspondence to Ana Gutiérrez, anagu@irnase.csic.es

Steroid ketones

Cholestan-3-one (compound F in **Fig. 1**) has a ketone in C3 instead of an alcohol and a single bond between C5 and C6. This ligand is not able to enter the binding pocket as well as compound A (**Fig. S5**). First the fraction of entrances by the C25 side is reduced (from 82% to 49%) and second the distance between the reactive hydrogen and the oxygen atom in cholestan-3-one is slightly longer (2.5 Å in A to 2.8 Å in F). This will have an effect in the reactivity of the compound and in particular will favor reaction at the most labile hydrogen (H25 being tertiary) since the number of reactive positions is considerably reduced (when compared to cholesterol). Interaction of the ligand in the active site is less favorable than cholesterol due to the fact that cholestan-3-one is incapable of hydrogen bonding to Glu245.

Cholesta-3,5-dien-7-one (compound H in **Fig. 1**) does not have the alcohol in C3, instead it has a ketone in C7 and an extra double bond at C3-C4. This molecule has an identical activity as cholesterol (57% substrate conversion vs. 64). Here the entrance by the C25 side is reduced (from 82% in cholesterol to 58% in cholesta-3,5-dien-7-one) probably due to the apolar nature of the steroid ring on the external side (C3) (**Fig. S6**). This also justifies reaction observed in the ring due to the presence of the double bond and C3 which can place itself correctly in the active site. However the hydrogen present on a carbon atom with an sp^2 hybridization has lower reactivity (similar to a primary carbon) which can explain the low percentage of product at the steroid ring.

Steroid hydrocarbons

Cholestane (compound J in **Fig. 1**) lacks the polar alcohol group in C3, which increases the fraction of entrance by this side of the ligand, but most importantly the bulkier saturated C5 and C6 (and consequent loss of planarity) impedes a suitable placement of the ligand in the binding site when it enters by C25. For this reason a low number of structures come close enough to the oxygen atom in cholestane (**Fig. S7**) which explains the low reactivity of this compound (cholesterol is converted by 64% while only 3% for cholestane).

Cholesta-3,5-diene (compound K in **Fig. 1**) has a very interesting reactivity due to the presence of two double bonds at C3 and C5. Also the lack of any polar group leads to a less favorable entrance by C25 (82% for A and 45% for K) (**Fig. 3**). This compound should also be compared to cholesta-3,5-dien-7-one as they only differ by the presence of a ketone group at C7 (**Figs. S6** and **S8**). This group has a considerable effect in reactivity. First it decreases the fraction of entrances by C3 (55% for K vs. 42% for H), thus increasing the conversion of the reactants to products (18% for K 57% and for H). Second, the more favorable entrance by C3 for cholesta-3,5-diene increases the fraction of hydroxylated products at the steroid rings. It is also interesting to note that many of these products are additions to the double bond.

Sterol esters

Cholesteryl acetate (compound M in **Fig. 1**) has almost the same structure as cholesterol but with an ester instead of a hydroxyl group in the C3. For this reason, the entrance to the protein by this side (**Fig. 3**) is favoured compared to cholesterol, while the opposite occurs at the C25 side (82% for cholesterol and 35% for cholesteryl acetate) (**Fig. 3**). Moreover, the binding position of the ligand in the C25 oxidation is no longer favoured by the hydrogen bond with Glu245 (**Fig. 4**).

Cholesteryl caprylate (compound O in **Fig. 1**) is similar to cholesteryl acetate but with a larger alkyl chain in the ester group. PELE simulations show that the ligand does not approach the heme group from the C25 side (**Fig. S9**) nor by the C3 (data not shown). The reason for this is the large hydrophobic chains that favor interactions with the protein to avoid solvent exposure. An unusual binding mode occurs for this molecule where a strong minimum energy structure is observed that hinders the correct placement of the molecule in the active site by either end.

Supplemental Figures

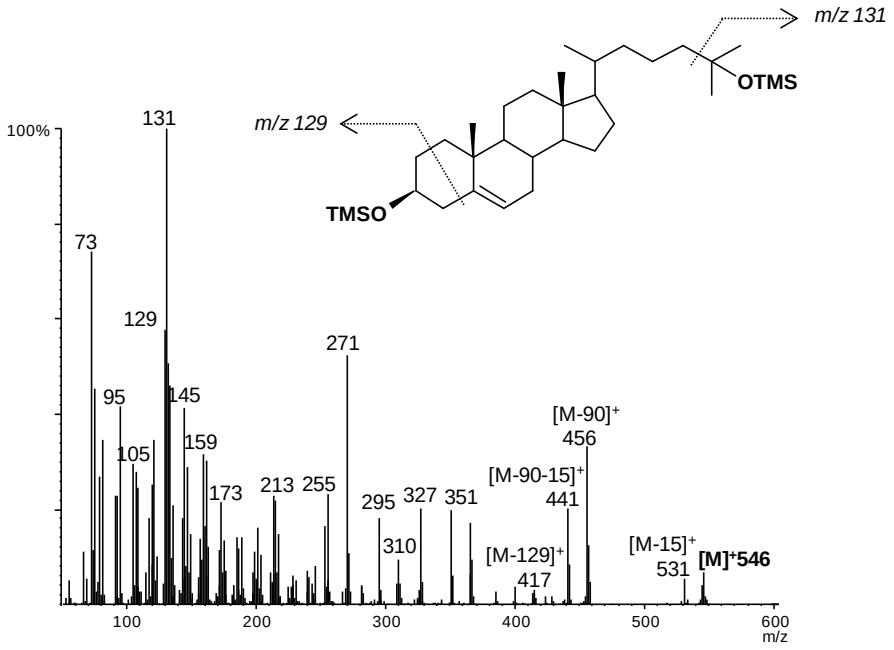

FIG S1 Mass spectrum of 25-hydroxycholesterol from peroxygenase reactions with cholesterol (see **Fig. 1**), as TMS derivative.

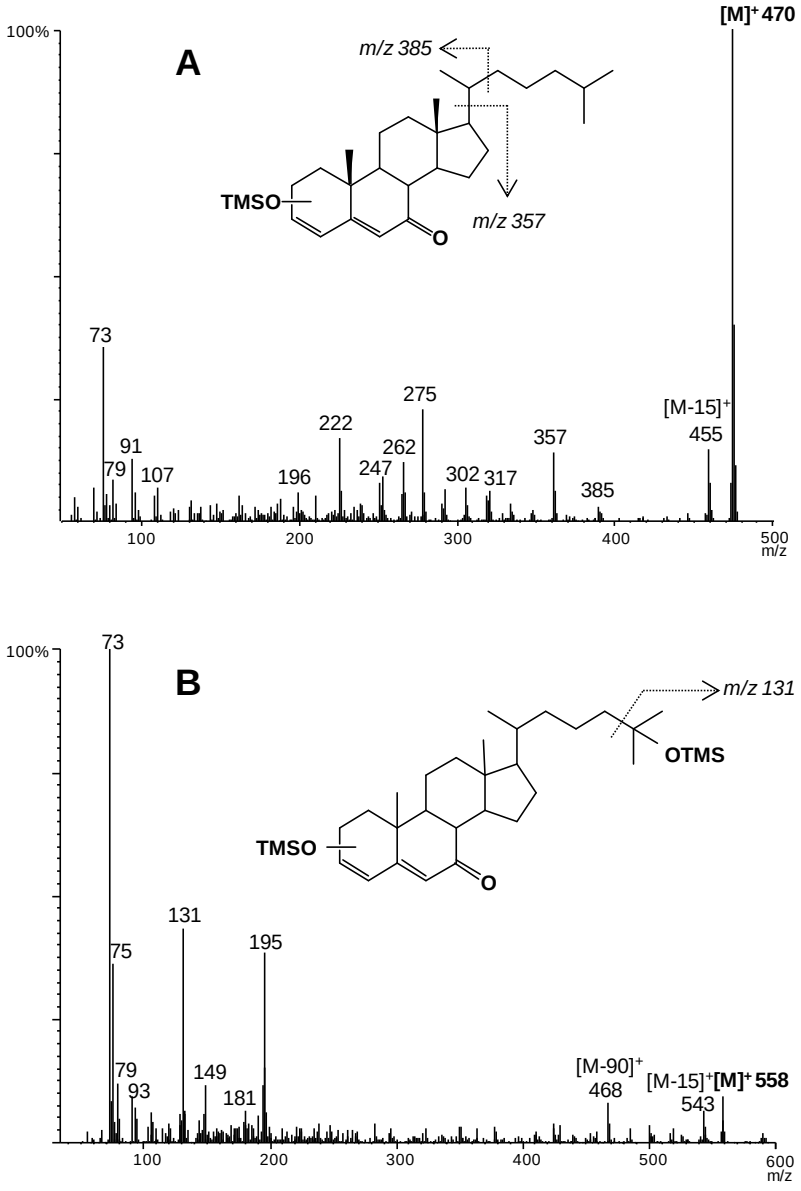

FIG S2 Mass spectra of x-hydroxycholesta-3,5-diene-7-one (**A**) and x,25-dihydroxycholesta-3,5-diene-7-one (**B**) from peroxygenase reactions with cholesta-3,5-diene-7-one (see **Fig. 1**), as TMS derivatives.

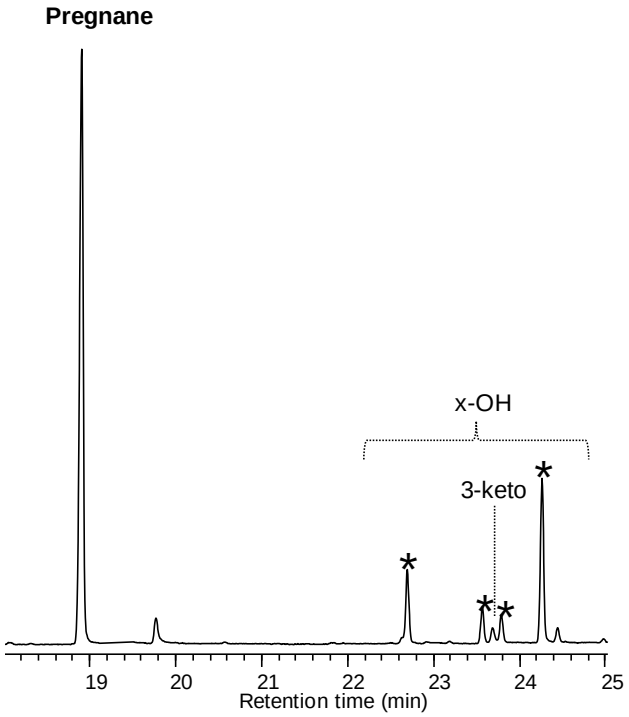

FIG S3 GC-MS analysis of the *Mro*UPO reaction (at 60 min) with pregnane (see **Fig. 1**) showing the remaining substrate and the monohydroxylated derivatives (x denotes the unknown position of hydroxylation in the ring).

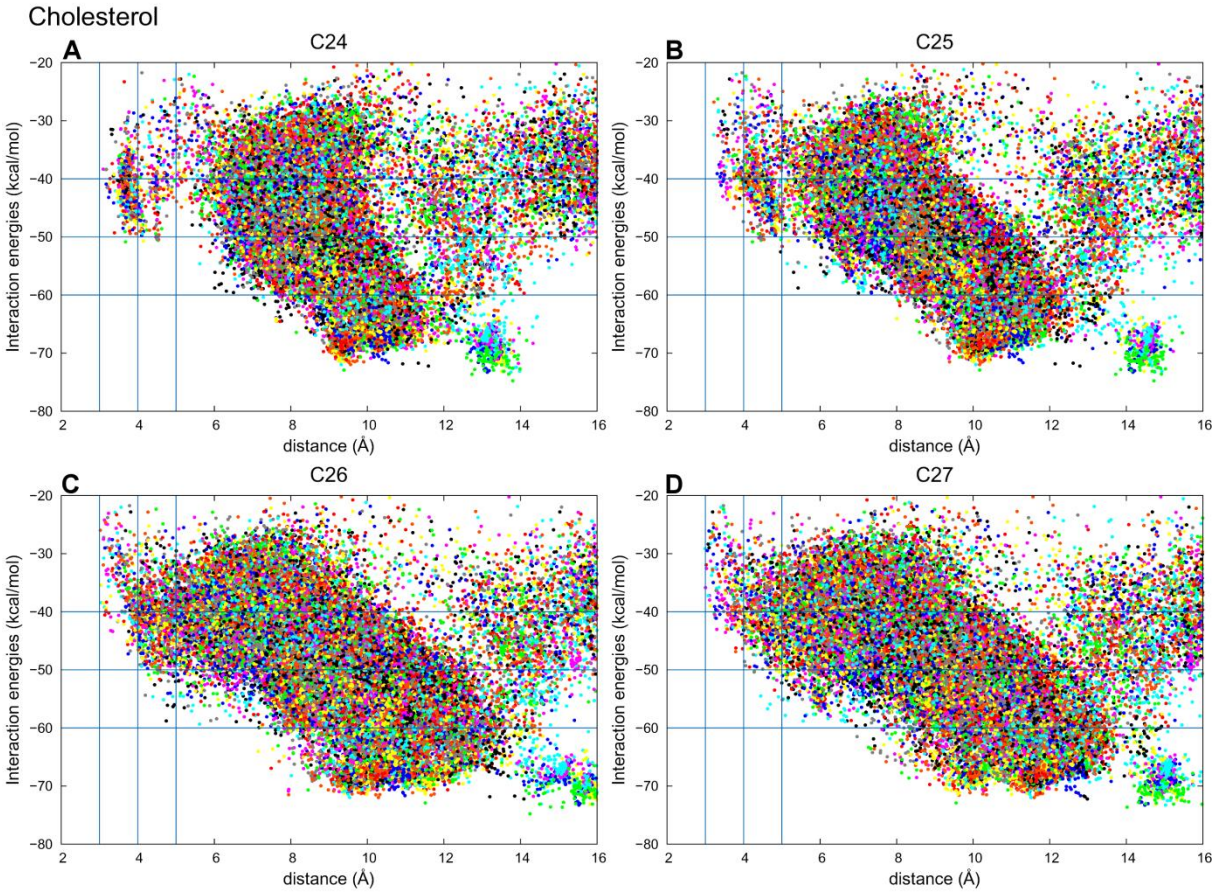

FIG S4 Results from PELE simulations for cholesterol (compound A in **Fig. 1**). The distances plotted correspond to the C24 (**A**), C25 (**B**), C26 (**C**) or C27 (**D**) atoms to the oxygen atom in *Aae*UPO compound I.

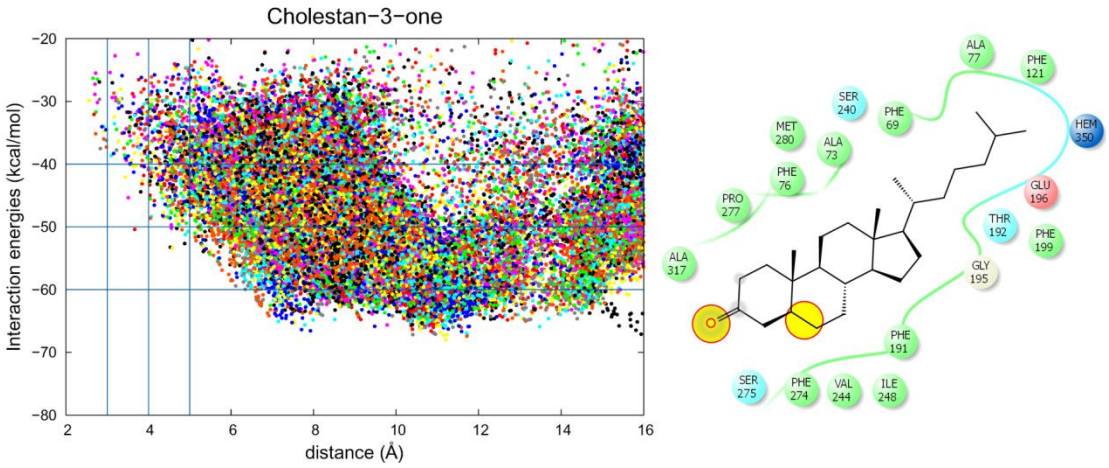

FIG S5 Results from PELE simulations for cholestan-3-one (compound F in **Fig. 1**) diffusion at the active site of the *Aae*UPO including: *(left)* Plots of the energy profile *vs.* the distance between the steroid H25 and the oxygen atom in enzyme compound I; and (*right*) Main interactions between cholestan-3-one and the enzyme in a representative structure in the binding site. The yellow circles identify structural differences relative to cholesterol.

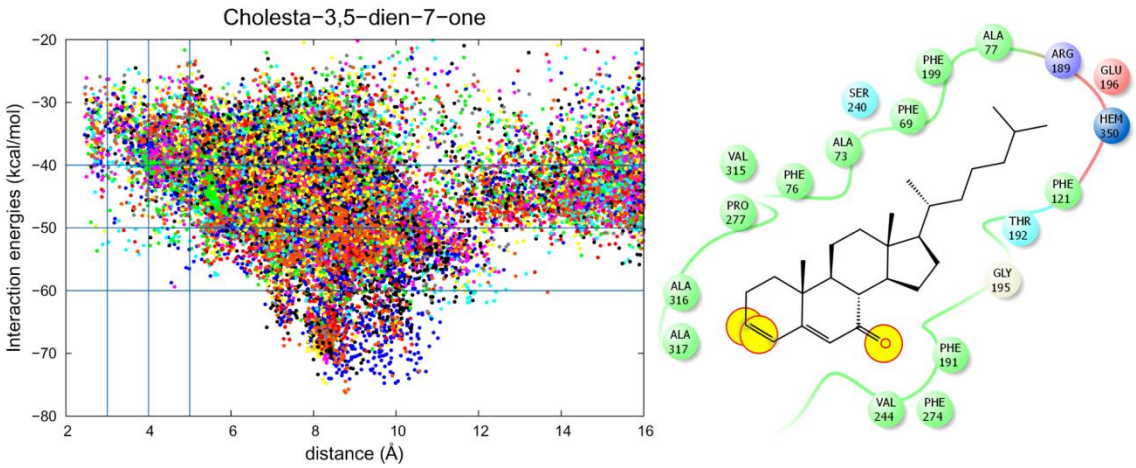

FIG S6 Results from PELE simulations for cholesta-3,5-dien-7-one (compound H in **Fig. 1**) diffusion at the active site with C25 approaching the heme cofactor of the *Aae*UPO, including: (*left*) Plots of the energy profile *vs.* the distance between the steroid H25 atom and the oxygen atom in enzyme compound I; and (*right*) Main interactions between cholesta-3,5-dien-7-one and the enzyme in a representative structure in the binding site. The yellow circles identify structural differences relative to cholesterol.

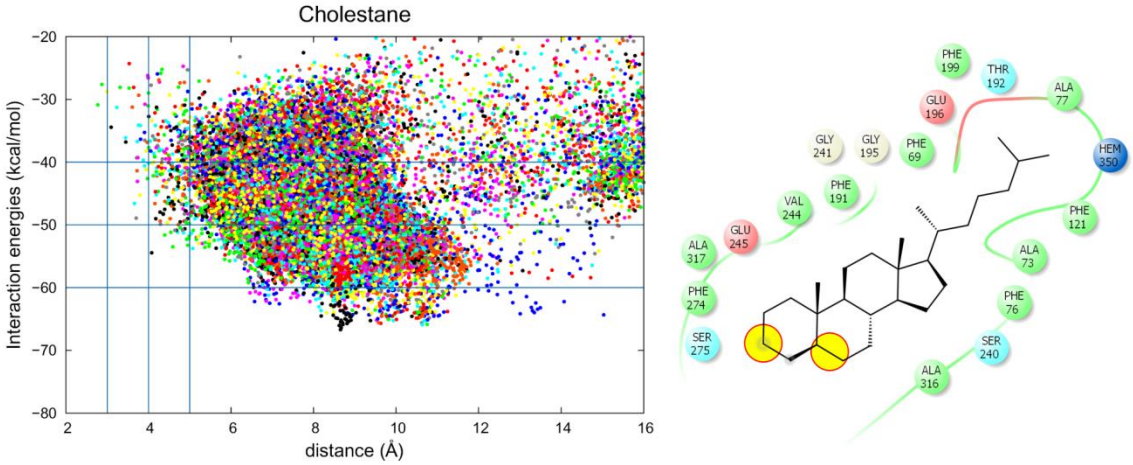

FIG S7 Results from PELE simulations for cholestane (compound J in **Fig. 1**) diffusion at the active site with C25 approaching the heme cofactor of the *Aae*UPO, including: (*left*) Plots of the energy profile *vs* the distance between the steroid C25 atom and the oxygen atom in enzyme cholestane; and (*right*) Main interactions between cholestane and the enzyme in a representative structure in the binding site. The yellow circles identify structural differences relative to cholesterol.

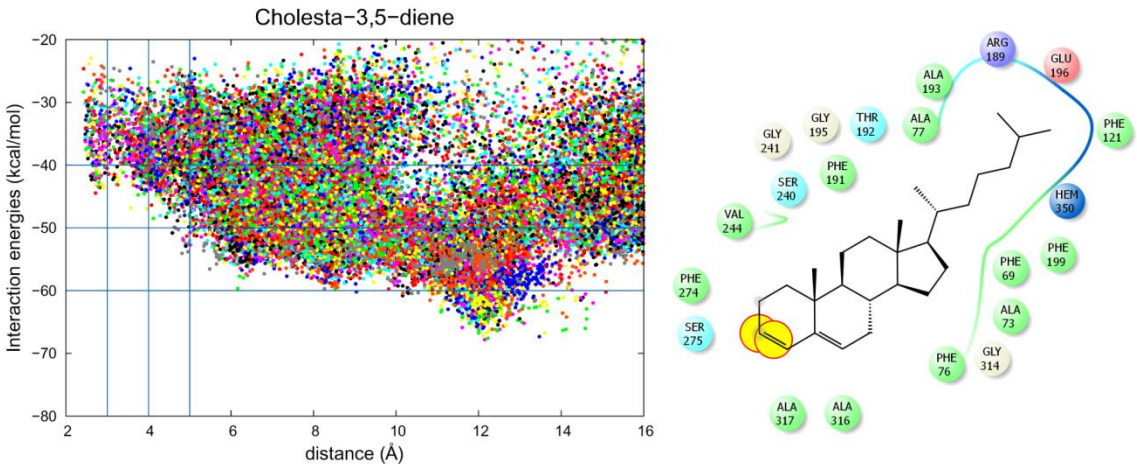

FIG S8 Results from PELE simulations for cholesta-3,4-diene (compound K in **Fig. 1**) diffusion at the active site with C25 approaching the heme cofactor of the *Aae*UPO, including: (*left*) Plots of the energy profile *vs.* the distance between the steroid H25 atom and the oxygen atom in enzyme compound I; and (*right*) Main interactions between cholesta-3,4-diene and the enzyme in a representative structure in the binding. The yellow circles identify structural differences relative to cholesterol.

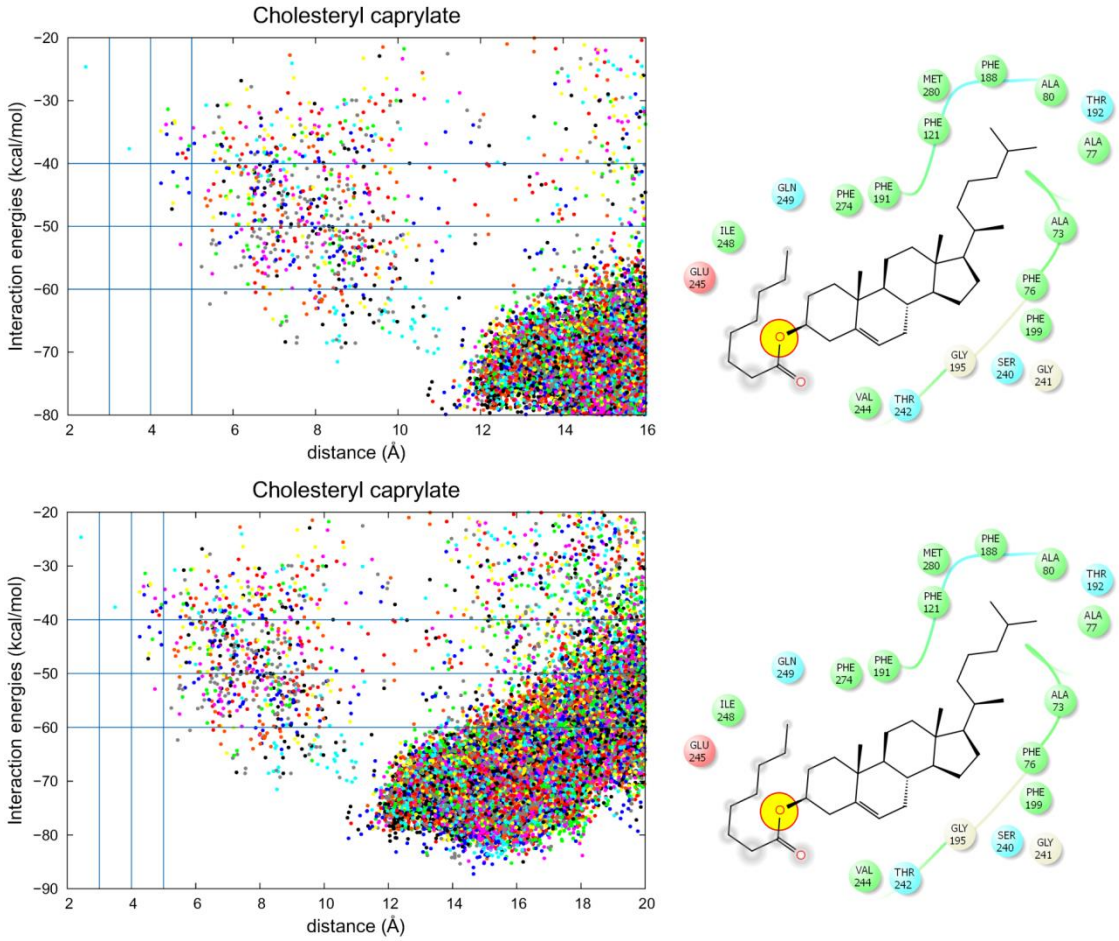

FIG S9 Results from PELE simulations for cholesteryl caprylate (compound O in **Fig. 1**) diffusion at the active site with C25 approaching the heme cofactor of the *Aae*UPO, including: (*left*) Plots of the energy profile *vs.* the distance between the steroid H25 atom and the oxygen atom in enzyme compound I; and (*right*) Main interactions between cholesteryl caprylate and the enzyme in a representative structure in the binding site. The yellow circles identify structural differences relative to cholesterol.